CHALMERS
UNIVERSITY OF TECHNOLOGY

CFD analysis of a novel rodent nose-only inhalation exposure chamber

SAMAN RAZAVI

Department of Chemistry and Chemical Engineering

CHALMERS UNIVERSITY OF TECHNOLOGY

Gothenburg, Sweden 2015

CFD analysis of a novel rodent nose-only inhalation exposure chamber

SAMAN RAZAVI

Department of Chemistry and Chemical Engineering

Chalmers University of Technology

SE-412 96 Göteborg

Sweden

Telephone + 46 (0)31-772 1000

Department of Chemistry and Chemical Engineering

CHALMERS UNIVERSITY OF TECHNOLOGY

Gothenburg, Sweden 2015

ABSTRACT

A first attempt of a study using Computational Fluid Dynamics (CFD) on an inhalation device for animals has been made in this thesis. This novel inhalation device has been developed at AstraZeneca R&D plant in Mölndal and its purpose is to deliver newly developed substance, as efficiently as possible, to the lungs of rodents. The primary focus of this thesis is to understand the physics of the system and the transport characteristics of the aerosol generated by the vibrating mesh nebulizer. It has been understood that the dispersed phase and the continuous phase have strong two-way momentum coupling close to the nebulizer and turbulence is generated due to this momentum coupling. The transport characteristics obtained from the CFD-simulations was compared with in vitro experiments and was confirmed to agree well with one other. Mainly through similar flow pattern characteristics, aerosol spread and aerosol velocity fluctuations when turbulence was generated. But further measurements is suggested to be done on the aerosol mass concentration before proper comparisons between the CFD-results and experiments can be made.

PREFACE

This Master of Science thesis has been performed by Saman Razavi, student at the master program Innovative and Sustainable Chemical Engineering at Chalmers University of Technology. This master thesis has been performed at the AstraZeneca R&D plant in Mölndal, Sweden with close collaboration with the department of Chemical Engineering at Chalmers University of Technology. The supervisors at AstraZeneca were Dr. Mikael Brülls and Dr. Johan Remmelgas and the supervisor/examiner at the university was Associate Professor Ronnie Andersson.

ACKNOWLEDGMENT

I would sincerely like to thank my supervisors Dr. Mikael Brülls, Dr. Johan Remmelgas and Associate Professor Ronnie Andersson for dedicated help and guidance whenever it was needed. I would also like to thank all the nice personnel I encountered at AstraZeneca R&D for making my time there fun and exciting.

TABLE OF CONTENTS

1 INTRODUCTION AND BACKGROUND

When treating diseases in the respiratory system, including asthma and chronic obstructive airway disease, it is of high interest to deliver the pharmaceuticals locally for effective action. AstraZeneca have several medicines for the treatment of respiratory diseases serving people all around the world and are continuously working to develop better and more effective medicines. In the development stages of potentially new pharmaceuticals, animal testing are made to observe how living mammals react to the newly developed substances. These substances are very expensive to produce and therefore you want as much substance as possible to reach the respiratory system of the animal, i.e. maximize the efficiency of the testing. However, the nasal cavity is the first line of defense in the respiratory tract that filters out the inhaled airborne particles, thus protecting the delicate airways [1]. Therefore there is of high interest to get a classification of droplets, small enough to pass the nasal filter, that get to the nose of the breathing animal [2].

1.1 Previous work

Cryan et al. [3] explained that strategies for enhancing systemic drug delivery via the lung are with new generation inhaler devices that produce much higher respirable doses. These include a new generation of liquid-spray devices that mechanically generate an aerosol, vibrating mesh technologies and dry powder inhalers that produce inhalable aerosols independent of the patient's inspiratory flow rate and volume. The method of aerosol administration is a key factor in the design of animal studies for drug delivery to the lungs and will impact the accuracy of the results obtained. The drug delivery can be through direct administration or passive inhalation, and these methods have their advantages and disadvantages.

The direct administration is, as its name implies, when a stainless steel tube is inserted directly in the airway of the animal and the substance is deposited locally. The main advantage with direct administration is that both small and relatively large doses of drugs can be delivered and that the dose delivered can be accurately measured. The disadvantage of the method is that it can cause significant stress in the subject, such as airway inflammation, and prevent uniform distribution throughout the lung. Experiments designed to deliver aerosolized drugs by passive inhalation employ exposure chambers that can be for whole-body, head-only and nose-only. Each exposure has its sets of advantages and disadvantages. An advantage with the whole-body exposure is that the animal is exposed without restrain, while the major disadvantage of this system is that a lot of the expensive substance goes to waste, i.e. is not inhaled. The main advantage with head-only and nose-only exposure systems is the reduction of pharmaceutical waste, however the disadvantage can be that the animal is stressed since the face or neck needs to be sealed.

The overall advantages with passive inhalation compared to direct administration is that the substance, which is of interest to reach the lungs, is more uniformly distributed and substance can be administrated to many animals simultaneously.

Another research article; Wu Y. et al. [4] present the development and design of a Radioactive Aerosol Generation and Inhalation System (RAGIS). The RAGIS was designed to mainly overcome problems of: low deposition of the radioactive aerosol in guinea pig lungs, production of excessive radioactive waste and heterogeneous distribution of aerosol in the guinea pig airways. The optimized exposure system is shown below in Figure 1 and it's a system for passive inhalation.

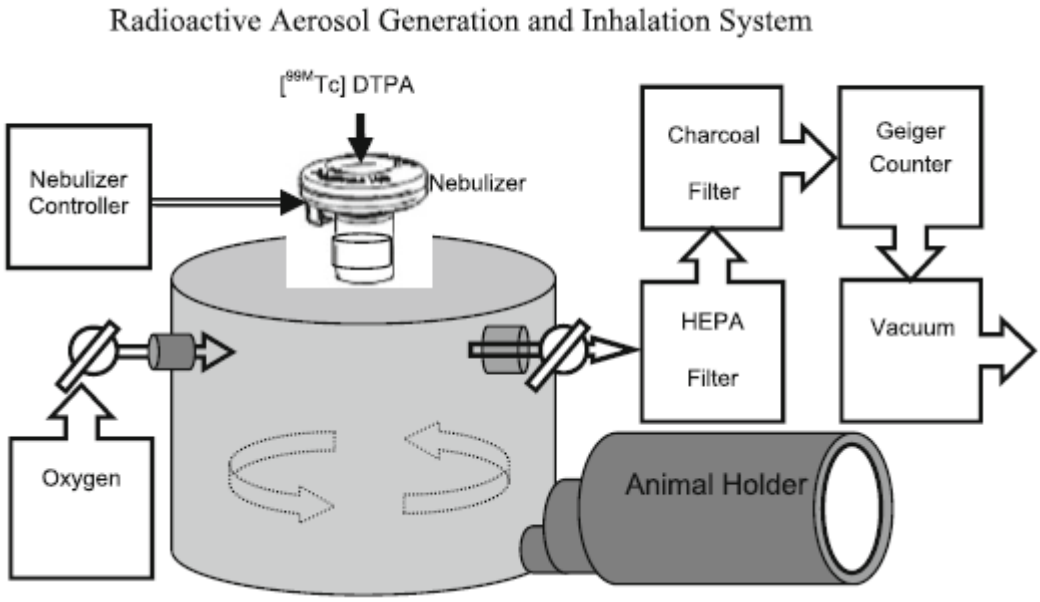

Figure 1. RAGIS equipment design.

The exposure chamber was filled with 95% oxygen and the animal was positioned in the animal holder with its nose towards the chamber. The animal was anesthetized so it breathes nicely and calmly with deep breaths. The aerosol was generated for 4 minutes and the animal was remained in the animal holder for an additional 1 minute, rebreathing the aerosol from the suspended cloud. At the end of the aerosol inhalation, the animal was removed from the system and the vacuum was turned and the waste aerosol was removed from the system. The development of the RAGIS system resulted in making the deposition efficiency in the lung tissues improving by a factor 20, when comparing to earlier studies of devices for passive inhalation [3]. The distribution of the substance in the lung tissue was also more homogeneous.

A device for nose-only inhalation exposure system for rodents have been developed at AstraZeneca, called Inhalation Device for Animals (IDA), to increase its efficiency. This device work, roughly speaking, in a way that the test compounds are administrated via passive inhalation in a novel closed exposure chamber which is used in combination with a vibrating mesh nebulizer to efficiently aerosolize and administer the compounds. Now, simulations in Computational Fluid Dynamics (CFD) on IDA are of high interest to hopefully get more understanding of the fluid dynamics of the system and the physics involved.

1.2 Objectives

The main objective of this thesis was to develop an understanding of the physics and fluid dynamics in an Inhalation Device for Animals (IDA) that has been designed at AstraZeneca. To assess that kind of understanding of the system, simulations in Computational Fluid Dynamics (CFD) was the main tool for calculations. These kinds of simulations haven't been done on this particular device previously. This thesis was therefore the first attempt of CFD-simulations.

The first objective was to design a CAD-model of the device that give a functioning and converging system when only air was flowing through the system, i.e. no dispersed phase involved. When that was achieved, particles could be added to the system and an understanding of the physics could gradually be built, i.e. questions like; is there any coupling between the phases (?), and if so, is the coupling significant? Another essential question to answer, when modeling the system, was if the flow regime is laminar or turbulent? When the physics between the dispersed phase and continuous phase were understood and the boundary conditions were well assumed, evaporation of the droplets could be taken into account. This would hopefully give an insight of the fluid dynamics of the droplet motion in the closed exposure chamber of IDA. Ultimately, the breathing pattern of the rodents could also be added to the system to study if this has any large influence on the system.

1.3 General constrains

- It is assumed that the substance that is sprayed into the system has the same physical properties as water.
- IDA is modeled as a axi-symmetric 2D-model

1.4 Method

The geometry of the device was drawn in ANSYS DesignModeler and its grid was created in ANSYS Meshing. The modeling and simulations was performed in ANSYS FLUENT v15. Before starting to model the system and making computational calculations, literature studies were made to get as much information and ideas as possible that might be applicable when modeling IDA. Then an assessment can be done about where the main focus should primarily be when an increased understanding of the system is aimed for.

For all the simulations, when a dispersed phase is involved, transient simulations were made. For the case when only a continuous phase is present, steady state simulations were performed. Since CFD-simulations have not been done on this particular device previously, the results of the simulations was mostly compared and validated by experiments (in vitro) and experience of the system.

2 DEVICE DESCRIPTION

The purpose of this section is to familiarize the reader with the IDA which is studied in this thesis. The purpose of the device and its different parts will be explained below.

2.1 Parts and design

In Figure 2, a CAD-drawing of the IDA is illustrated and it was designed in ANSYS DesignModeler. The purpose of this CAD-drawing is for illustrative purposes only and it is a representation of the real device.

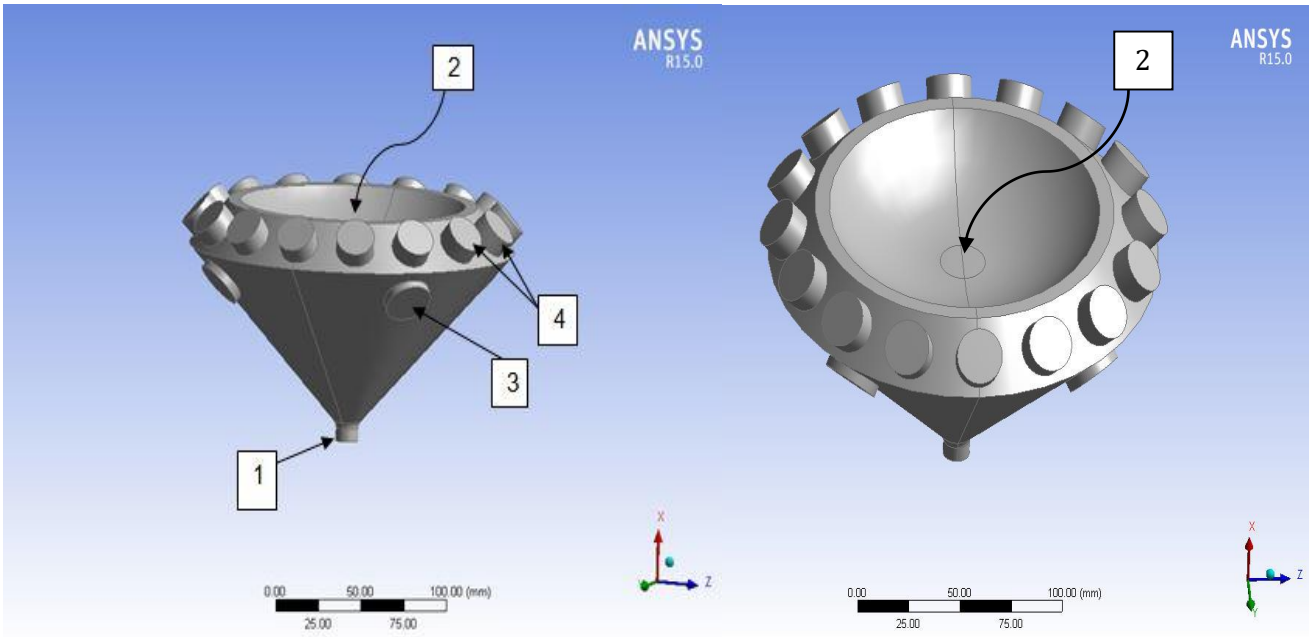

Figure 2. Design of the IDA.

The different parts are numbered in Figure 2 for short explanations. Part (1) on the bottom of the device is the inlet pipe for dry air, the air will act as a carrier gas to ultimately administrate the substance droplets to the rodents and at the same time act as essential air for the living animal and carbon dioxide poisoning can be prevented. Part (2) is located in the center of the concave half circle on the top part of the IDA, this is the vibrating mesh nebulizer. Its purpose is to generate a very fine aerosolized spray which is aimed to be dosed to the rodents, more detailed information about the vibrating mesh nebulizer is to come further down in this chapter. (3) is an outlet from the cone-shaped closed exposure chamber were the rodent is placed to inhale the aerosolized substance. Two outlets can be seen in the Figure but there are two on the other side as well (four in total). The rodents are placed at these outlets with "animal holders", an example of an "animal holder" can be seen in Figure 1. Number (4) in Figure 2 is 16 outlets with filters which capture the substance that doesn't end up in the rodent.

It was recognized that the boundary condition for the vibrating mesh nebulizer and the physics that evolve around this unit is crucial for correct modeling of the system and is therefore of outmost importance to be understood. This was accomplished with the assistance of CFD and experimental (in vitro) guidance and will be discussed further in section 3.2.1. The experimental guidance was made over a simple and transparent cylinder and the CFD simulations were also made for this geometry. This simple cylinder is illustrated in Figure 3.

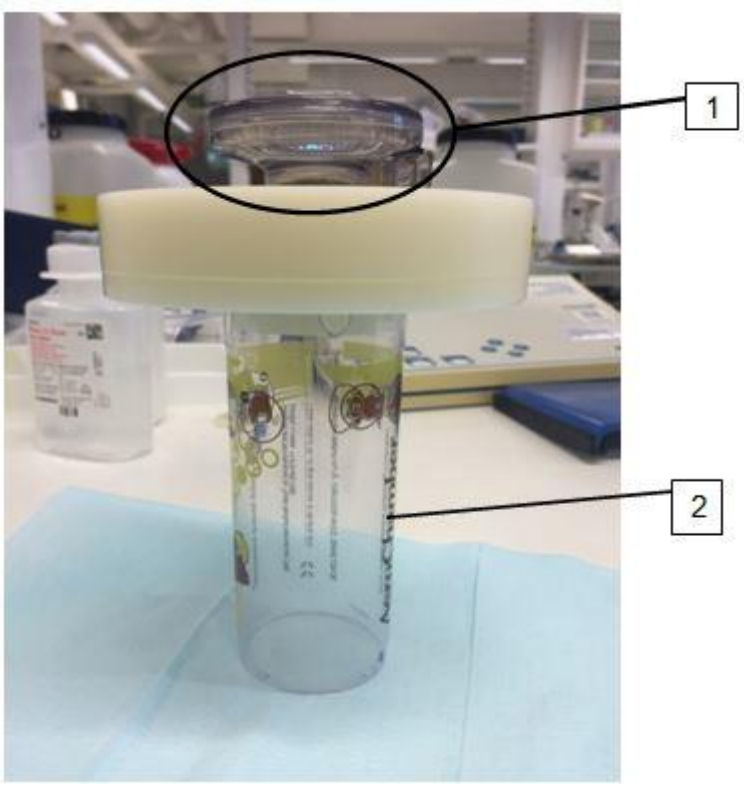

Figure 3. Cylindrical geometry that will be used to do CFD- and experimental analysis to enhance understanding of the vibrating mesh nebulizer.

The parts in Figure 3 are numbered for explanation. Part (1) is the Aeroneb® Lab vibrating mesh nebulizer and part (2) is the cylindrical shaped body were the aerosol will flow through.

2.2 Vibrating mesh nebulizer

The vibrating mesh nebulizer, Aerogen® Lab, used in IDA creates a fine particle, low velocity aerosol optimized for targeted delivery through the lungs. It's designed to produce an aerosol from a drug in liquid format without damaging or altering the compound's molecular integrity or altering the concentration. The vibrating mesh technology is a patented high performance aerosol technology, called Vibronic™. It's a nebulizer with an aperture plate of about 10mm in diameter containing over 1000 precision-formed holes, surrounded by a vibrating element, called piezoelectric. When energy is applied to this vibrating element, the aperture plate start to vibrate at a high frequency, over 128 000 times per second, and during each pulse the aperture plate is displaced about 1µm. Due to this rapid vibration, the aperture plate will act as a micro pump, drawing liquid through the holes to form consistently sized micron droplets [5]. The droplet size for this particular nebulizer is about 5µm. Figure 4 is a good illustration of the operational mechanism of vibrating mesh nebulizers.

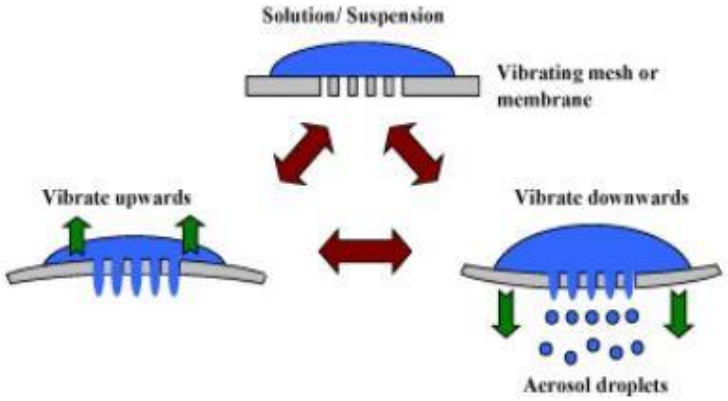

Figure 4. Operational mechanism of a vibrating mesh nebulizer adopted from [6].

2.3 Geometry and grid

The first step for solving a CFD problem is by drawing the geometry of the system that is to be simulated for. In this thesis ANSYS DesignModeler is used to do the CAD-drawing of IDA and the cylinder. When the modeling of the geometry is done, the domain is discretized into a number of computational cells using the finite volume method. This is known as; meshing or grid generation. It is important that the grid have a fairly good quality to achieve convergence and prevent inaccurate results, for that reason the quality of the grid is evaluated prior to simulation [12]. Aspect ratio and skewness are two important factors that are evaluated to determine the quality of the grid generated for respective geometry.

2.3.1 Geometry of IDA

As a preliminary design and study of IDA it was decided that a 2D-model would be satisfying enough for the future simulations. The 2D-geometry can be seen in Figure 5, and it represents a cross-section of the 3D-geometry, see Figure 2. When going from 3D to 2D, the outlets of IDA are modeled as continuous vents going all around the device. The dimensions of the outlet vents are determined by knowing the total area of the actual outlets (in the 3D model) and scaling it so a continuous vent is obtained, i.e. the total area of respective outlet has the same total area as the respective continuous vent. In Figure 5, the axi-symmetric 2D-geometry of IDA is presented with its grid.

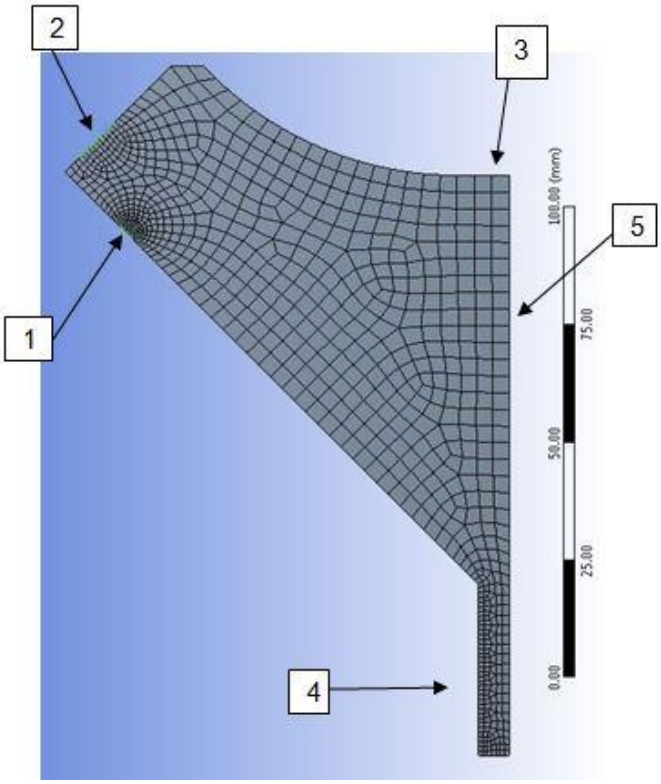

Figure 5. Axi-symmetric 2D-geometry of IDA.

The parts in Figure 5 are numbered for explanation. (1) shows the continuous vent that represents the outlet for rodents, (2) shows the continuous vent that represents the outlet for filters, (3) indicates the location of where the nebulizer is positioned, (4) is the inlet pipe for air and (5) is the symmetry axis. A fine grid with 1868 elements was generated. The aspect ratio is recommended to be below 5 and the maximum skewness should be below 0.95 and the average skewness below 0.33 [12]. The fine grid for this geometry fulfills these recommendations and they are presented in Table 1.

Table 1. Details for determining grid quality.

Measurement	Min.	Max.	Average
Aspect ratio	1.0	4.55	1.12
Skewness	1.3E-02	0.8	8.53E-02

2.3.2 Geometry of cylinder

This 2D-geometry presented in this section represents the cylinder that is illustrated in Figure 3.

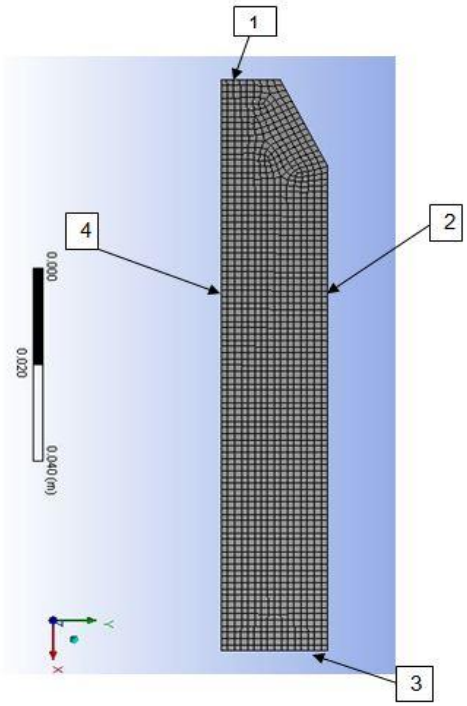

Figure 6. 2D-geometry of the cylinder.

The parts in Figure 6 are numbered for explanation. (1) is the location of where the dispersed phase is injected into the system (nebulizer), (2) is the walls of the cylinder, (3) is the outlet of the cylinder and (4) is the symmetry axis. A fine grid was generated with a total of 1434 elements. The aspect ratio and skewness were studied for this case as well and are presented in Table 2.

Table 2. Details for determining grid quality.

Measurement	Min.	Max.	Average
Aspect ratio	1.0	1.34	1.03
Skewness	1.3E-10	0.38	1.54E-02

3 MODELING APPROACH

When approaching this problem of understanding the fluid dynamics in the device and the physics between the continuous phase and dispersed phase etc., it is necessary to take on the problem step wise and gradually increasing the understanding of the whole system.

3.1 Flow characterization in IDA

The first step, when approaching the whole problem of this inhalation device, was to get a good understanding of the fluid dynamics in the system without a dispersed phase involved. It is of high interest to determine the flow regime in the system to be able to know in which direction to go when modeling the system, i.e. if the flow is laminar or turbulent for instance. The Reynolds number is often used to determine the flow regime, i.e. if the flow is laminar or turbulent. This dimensionless number represents the ratio between the inertial forces and viscous forces, see equation (1);

$$Re = \frac{d * u}{\nu} \quad (1)$$

In equation (1) the parameters are; characteristic diameter (d), velocity (u) and kinematic viscosity (ν). When calculating the Reynolds number for the inlet pipe of IDA, a dimensionless number of about 14 were obtained. A low Reynolds number was expected since the air velocity throughout the inlet pipe is very slow and the pipe is rather narrow. For pipe flows, the Reynolds number should be greater than ~2100 to go from laminar to turbulent flow [12]. When this laminar flow from the inlet pipe will enter the cone shaped closed exposure chamber of IDA the volume of the system is increased drastically. The question now remains; will the flow be expected to stay laminar? By analyzing the expression for the Reynolds number, see equation (1), it can be determined that it is linearly dependent of the characteristic diameter, i.e. as the diameter is increased the Reynolds number will increase. However, it is essential to keep in mind that the velocity of the fluid flow is dampened quadratically by the characteristic diameter, see equation (2);

$$u = \frac{(volumetric\ flow\ rate)}{\frac{\pi d^2}{4}} \quad (2)$$

It is therefore assumed that the velocity (u) will be more affected by an increase in diameter (slowed down) of the system which will lead to an even lower Reynolds number in the cone shaped closed exposure chamber of IDA, i.e. fluid is assumed to stay laminar.

When air flow through the inlet pipe and there are “no-slip” conditions at the walls, a parabolic velocity profile is expected to develop. The distance it takes from the pipe entrance to get a fully developed parabolic flow is called the entrance length, symbolized as L_e. The entrance length required to achieve a fully developed velocity profile for laminar flows is calculated with equation (3);

$$\frac{L_e}{D} = 0.0575Re \quad (3)$$

Where D, represents the inside diameter of the inlet pipe [13]. The L_e was calculated to be ~10mm. It is due to this information that a ~30mm inlet pipe was designed for the 2D-geometry of IDA, to assure that a parabolic profile is developed, see section 2.3.1. When modeling this system, laminar flow is assumed and solved for. From a numerical point of view, the classical form of Navier-Stokes equation is solved without applying any time averaging.

3.2 Multiphase flow modeling

When the substance from the vibrating mesh nebulizer is sprayed into a domain that is wished to do CFD-simulations for, it becomes a multiphase problem. To predict particulate two-phase flows, two main approaches are possible. One treats the fluid phase a continuum (Eulerian-framework) and the dispersed phase as individual particles (Lagrangian-framework). This approach, which predicts the particle trajectories in the fluid phase as a result of forces acting on particles, is called the Eulerian-Lagrangian (E-L) approach [14]. The other approach treats the dispersed phase as a continuum and solves the appropriate continuum equations for the fluid and particle phases and is called the Eulerian-Eulerian (E-E) approach. This approach is mainly applicable for dense flows. The more interested reader is referred to [14] and [12] for more detailed description about these models.

3.2.1 Vibrating mesh nebulizer as boundary condition

A dispersed phase is introduced in the inhalation device when the vibrating mesh nebulizer start to spray the newly developed substance into the closed exposure chamber, which is aimed to be dosed to the rodents. Literature studies have been made on the subject of using CFD for modeling and design of inhalers were a nebulizer is used to aerosolize the substance in association with dosage to lungs. However, none of the inhaler devices that have been studied with CFD previously are similar to the inhalation device (IDA) that is to be studied in this thesis.

While CFD is used comprehensively in traditional engineering to guide the design of equipment, it has only recently seen increased use in the design for inhalers for therapeutic delivery of aerosols into respiratory tract [8]. But there are challenges ahead. According to Ruzycki C.A et al., Longest P.W et al., Wong W et al. and Ilie M et al. the use of CFD for inhaler design is relatively limited due to extreme complexity of the coupled fluid and aerosol generation [7-10]. Due to these complications, relatively few CFD studies have been performed on nebulizers [8].

As a result of the complex nature around the vibrating mesh nebulizer the primarily focus, in this thesis, was to understand the boundary conditions and the physics that evolve around this unit. Longest P.W et al., Wong W et al., Hindle M et al and Ruzycki C.A et al. all agree on the fact that the CFD-simulations should be done concurrently with experimental analysis. That will primarily help validating the CFD-simulations but it will also significantly enhance the knowledge and understanding of the experiments [7-9][11]. Therefore, careful experimental studies of the aerosolized substance from the vibrating mesh nebulizer should be made alongside the CFD-studies. Since there are a lot changes in the flow characteristics over very small time scales when the aerosol is generated, it is quite difficult to study flows and movements with the naked eye. A high speed camera was therefore used to simplify the analysis of the aerosol spray with the naked eye; this is also done by Wong W et al. in the development stages of nebulizers [9]. Since CFD-simulations was made concurrently with visual guidance to enhance the understanding of the vibrating

mesh nebulizer, both of these cases was made over a simple, transparent cylinder geometry which was presented in section 2.1.

Not enough information about the vibrating mesh nebulizer is supplied by the manufacturer to help getting any initial awareness about the boundary conditions and physics involved about this unit in particular. Therefore an iterative process to match the CFD results with the experimental results was performed. This iterative approach was also performed by Longest P.W et al. [7]. When the understanding of the system, in the cylinder, is thought to be well judged, then particles can be introduced into the IDA-geometry.

3.2.2 Volume fraction

It is of interest to be aware if ones multiphase system is mainly dense or dilute when going about choosing an appropriate multiphase model. The volume fraction, α_d, can be calculated to determine how much of the local volume is occupied by the dispersed phase [12], see equation (4).

$$\alpha_d = \frac{\sum_{i=1}^{N_d} V^i}{V} \quad (4)$$

where V^i is the volume occupied by the dispersed phase and V is the local volume of interest. With rough estimates, a α_d have been calculated for the case when substance is sprayed into the cylinder. This calculation can be followed in more detail in A.1. An extreme case is to investigate the α_d in a control volume very close to the nebulizer. A control volume with a minimum volume of about $1 \cdot 10^{-9}\,\mathrm{m}^3$ is considered and as elaborated in A.1 a α_d of $8 \cdot 10^{-3}$ is obtained. According to Figure 7, a α_d of $8 \cdot 10^{-3}$ is borderline dense suspension. That there is dense suspension very close to the nebulizer is assumed and the modeling of this will be explained further in section 3.2.7. But as the spray is transported further down into the cylinder and spread over a larger control volume, it is assumed that the volume fraction of the dispersed flow will go over to a dilute suspension.

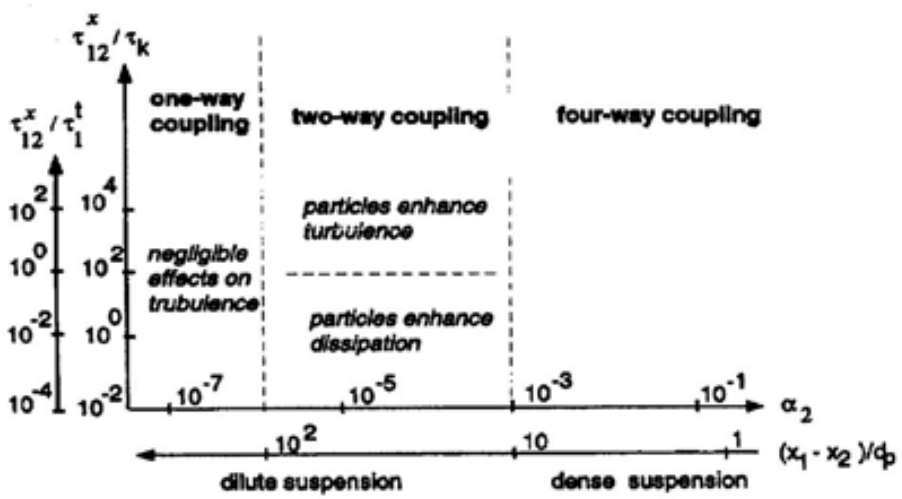

Figure 7. Regimes of dispersed two-phase flow coupling as function of particle volume fraction adopted from Elgobashi [15].

3.2.3 Choice of a suitable multiphase model

As mentioned, when having a dense flow of particles the E-E approach is applicable and the main idea behind modeling a particulate phase as a fluid is to get a less computationally expensive system. When a continuous field is modeled of the particulate phase, an averaging is made over the particles thus giving no information about the individual particles. Fundamental assumptions for the E-E model are that the particles are of identical size, smooth, rigid, spherical with instantaneous binary contact [16]. As was shown, the volume fraction in our system of interest is expected to be mainly in the dilute regime and therefore the E-E is not appropriate in this case. When modeling a polydisperse particle flow with E-E, it results in several coupled momentum equations which can lead to an unstable system. That makes another reason that E-E shouldn't be the way of modeling this system. However, E-L can handle polydispersity more easily and is good for dilute flows and mainly due to these factors, E-L was chosen as the appropriate multiphase model. All literature studies that have been made, prior to choosing a multiphase model for this system in particular, use the E-L approach when modeling nebulizers as well. That is another indication that the Lagrangian framework is the traditionally accepted method for these types of multiphase problems.

3.2.4 Eulerian-Lagrangian model

The continuous phase is modeled in the Eulerian framework and the dispersed phase is modeled in the Lagrangian framework, hence the name. In the E-L modeling approach, the continuity and the momentum equation are solved for the fluid phase and the equation of motion is solved for the dispersed phase. Below, the governing equations, (5) and (6), for the continuum phase are presented when tracking individual particles;

$$\frac{\partial}{\partial t}\left(\alpha_f \rho_f\right) + \nabla\left(\alpha_f \rho_f \boldsymbol{u}_f\right) = 0 \ (+S_{mass}) \quad (5)$$

$$\frac{\partial}{\partial t}\left(\alpha_f \rho_f u_f\right) + \nabla\left(\alpha_f \rho_f \boldsymbol{u}_f u_f\right) = -\alpha_f \nabla p_f - \nabla\left(\alpha_f \tau_f\right) - S_p + \alpha_f \rho_f g \quad (6)$$

The continuity equation, (5), describes the material balance over a fluid element. The term S_{mass} is a source term that is taken into account if there is exchange of mass between the particles and the fluid, for instance when evaporation takes place. The term S_p, in equation (6), is the source term that is taken into account when there is momentum coupling between the phases. This source term represents the momentum impact from the discrete phase on the continuous phase, e.g. when one-way coupling is assumed this source term is equal to zero. How the particles are modeled is explained in section 3.2.5.

Overall, the E-L model is a very accurate model since it tracks particles individually. But it is also due to this fact that this model has its limitations. When it comes to systems with too many particles, the simulations become computationally very expensive. It is difficult to say how many particles that can be tracked exactly, since it depends on the computational power available and the degree of physical phenomena included in the simulations. But a rough estimate is that a couple of hundred thousand particles is usually the limiting amount of particles when modeling with E-L on today's average computational power.

3.2.5 Modeling of individual particles

The equation of motion is solved for when modeling the movement of an individual particle. The equation of motion is modeled as sum of forces acting on the particle and the equation is written;

$$m_p \frac{d\boldsymbol{u_p}}{dt} = \sum F_i \quad (7)$$

Forces that could be included in the model are;

$$\sum F_i = F_{Drag} + F_{Lift} + F_{Added\ mass} + F_{History} + F_{Brownian} + F_{Therm} + F_{Press} + F_{Bouy} + F_{turb} \quad (8)$$

Some of these forces will now be explained further, the more interested reader is referred to [12] for more detailed explanation of all the forces.

3.2.5.1 Forces acting on the individual particles

Drag force

For a single particle the drag force is expressed as;

$$F_D = \frac{1}{2}\rho_f C_D A_{sphere}(u_f - u_p)^2 \quad (9)$$

The drag coefficient, C_D, varies as the Re_p is increased and this is done with successful results, i.e. the drag coefficient is well assumed for higher Re_p as well [17].

Lift force

This force arises due to velocity gradients in the flow. The Saffman lift force is due to a velocity gradient in the normal direction to the flow and the Magnus lift force is due to rotation of the particle.

Added mass force

This force arises due to acceleration or deceleration of the fluid surrounding an accelerating or decelerating particle. A fraction of the surrounding continuous phase follow the particle, increasing the particle virtual mass. Its expression is;

$$F_A = \frac{1}{2} m_p \frac{\rho_f}{\rho_p} \frac{d}{dt}(uf - up) \quad (10)$$

History force
This force describes how long it takes to develop a new boundary layer around a particle after it has been accelerated or decelerated.

Brownian force
The Brownian motion force is important only for very small particles (smaller than 1μm) and is modeled as a random motion.

Thermophoretic force
The thermophoretic force is of importance when there exist a temperature gradient in the flow. "Cold" particles and fluid will then diffuse to warmer parts of the flow and vice versa.

Pressure gradient force
This force arises due to pressure gradients in the system and it is often decided if this force should be taken into account by studying the size of the particles, it affects larger particles more than smaller particles. The expression for this force is;

$$F_p = m_p \frac{\rho_f}{\rho_p}\left(\frac{Du_f}{Dt} - g\right) \quad (11)$$

In this study many of the above mentioned forces can be neglected. Regarding the density ratio between the continuous phase and dispersed phase, (ρ_f/ρ_d), it is very small since the system of interest is modeled with air and water. Therefore the history-, added mass- and pressure gradient force are neglected. The particles are micro-sized and the Brownian force will be neglected, and since there isn't any temperature gradient in the system the thermophoretic force can be neglected as well. Velocity gradient may be expected very close to the nebulizer inlet but mainly not present in the system overall and the lift force is therefore chosen to be neglected. Consequently, drag force and gravity force will be the forces that will be included in the equation of motion for particles.

3.2.6 Phase coupling
One-way coupling means that the particles are not affecting the fluid flow, the particles however are affected by the motion of the fluid. In *two-way coupling*, the behavior of the particles has an impact on the fluid and vice versa. In both of these cases, particle-particle interactions are neglected. For *four-way coupling*, particle-particle interactions are also included.

The Stokes number (St) is a measure of coupling between phases. It is defined as the ratio between the particle relaxation time (τ_{xp}) and the characteristic time scale of the fluid phase (τ_f);

$$St = \frac{\tau_{xp}}{\tau_f} \quad (12)$$

For simple flow at low Reynolds numbers the particle relaxation time is calculated from;

$$\tau_{xp} = \frac{\rho_p d_p^2}{18\mu_f} \quad (13)$$

The value obtained from equation (14) in our case is about $7.6 \cdot 10^{-5}$ seconds. A detailed calculation of the τ_{xp} is presented in A.2. The time scale of the flow field is not known a priori but since the flow field is expected to be laminar when the particulate phase is not present, as explained in section 3.1, the time scale of the flow field is expected to be much larger than the particle response time. As such, the Stokes number can be expected to be much less than unity, St<<1, i.e. the dispersed phase follows the changes in the fluid field instantaneously. This is also intuitively justified since the particles in the system will be very small (average 5μm). This indicates a one-way coupling. But when solving the equation of motion, (8), numerically when drag force and gravitational force is taken into account, the dispersed phase injected from the nebulizer reach a terminal velocity of approximately $6 \cdot 10^{-3}$ m/s instantly. See A.3 for a detailed calculation of the terminal velocity. It can easily be concluded that this is not what is observed when visualizing the droplet velocity from the nebulizer. Eslamian et al. have measured the aerosol velocity about 2 cm from the nebulizer and a velocity of about 2 m/s was noted [18], which is further reason for not believing one way coupling is taking place close to the nebulizer. We need to remind ourselves that the volume fraction, of the dispersed phase, is quite high close to the nebulizer and therefore higher order coupling should be expected. One characteristic measure that is important in this case is the π_{mom} which is a measure of the momentum phase coupling, see equation 14.

$$\pi_{mom} = \frac{\overline{\rho_d}/\overline{\rho_c}}{1 + St} \quad (14)$$

Where $\bar{\rho}_d$ is the apparent density of the dispersed phase and $\bar{\rho}_c$ is the apparent density of the continuous phase. Since the apparent density of the dispersed phase is high close to the nebulizer it results in a high π_{mom} which proves a strong two way momentum coupling. At this stage the drag force dominates the momentum flux of the continuous phase.

The physical phenomena, which is also explained by Longest P.W et al., that is taking place is that the vibrating mesh nebulizer spray entrains surrounding air resulting in an induced flow that propels the droplets beyond their individual stopping distances [7]. That means that the droplets significantly influence the momentum on the surrounding air and therefore two-way coupling should be considered. This heavy coupling between the phases was already mentioned briefly in section 3.2.1, and its reason was explained here.

3.2.7 Particle distribution

As mentioned in section 2.2, the vibrating mesh nebulizer pumps in droplets of ~5µm. But due to the quite high volume fraction of dispersed phase very close to the nebulizer the suspension is classified as dense, see Figure 7. Because of this dense suspension, it's believed that particle break up and agglomeration takes place very close to the nebulizer. This results in a distribution of droplet sizes in the aerosol. The high frequency of the aperture plate that injects the substance is also believed to have such impact on the droplets that break up take place which results in a droplet distribution. Close measurements of the particle distribution in the aerosol have been made at AstraZeneca. In this thesis it will be assumed that the particle distribution is constant when injecting droplets into the system. This assumption will drastically decrease the computational cost for the simulations since particle break up and collisions will not be needed to be taken into account. This assumption is accepted in this case since this is mainly a preliminary CFD study of the nebulizer and the transport of the particles in the cylinder is of main interest. ANSYS FLUENT has a built in particle distribution set up called Rosin-Rammler particle distribution. The more interested reader is referred to [19] for detailed information about this distribution. The measured particle distribution has been matched with the Rosin-Rammler distribution, see Figure 8.

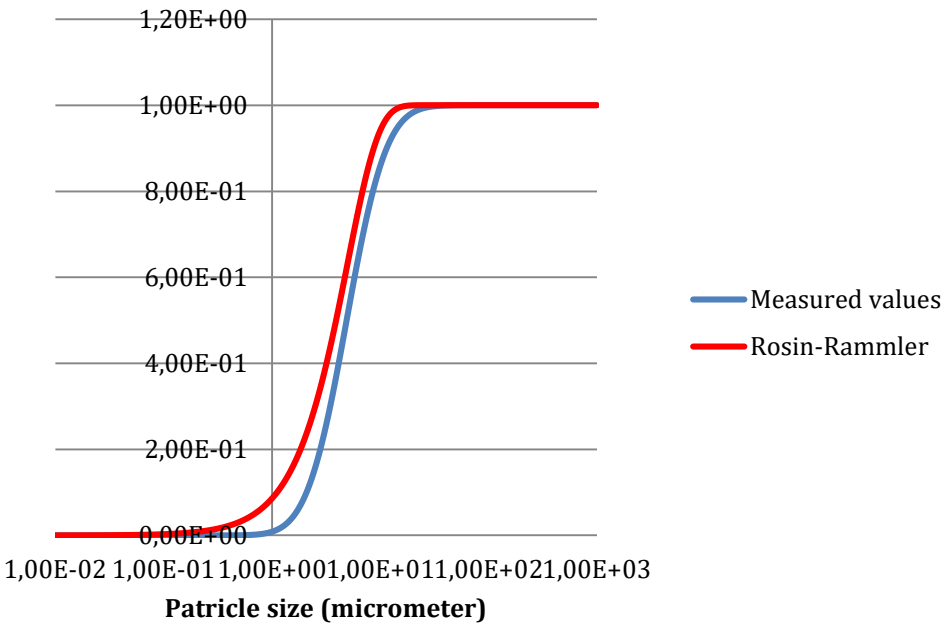

Figure 8. Cumulative distribution function curves for measured values and Rosin-Rammler function values with a spread parameter of 1.5 and a mean diameter of 5µm.

To best fit the Rosin-Rammler curve to the measured values, the least square method was used. This was made for three different spread parameters, see table 3, with a mean particle size of 5µm. Since a spread parameter of 1.5 gave the highest value of 0.996343 this was the one chosen when modeling in FLUENT. Since only three different spread parameters were investigated, a thorough work for optimization was not made. However, this is assumed to be good enough for this preliminary study.

Table 3. Least square value between Rosin-Rammler and measured values curve for different spread parameters.

Spread parameter	Least square method value
1.0	0.991060
1.5	0.996343
2.0	0.996003

The Rosin-Rammler function seems to be more skewed towards smaller particles, i.e. it overestimates the small particles and underestimates the larger particles for a fixed mean value. That is why the Rosin-Rammler curve is slightly shifted to the left.

3.2.8 Turbulence modeling

According to Longest P.W et al., Ruzycki C.A et al, Wong W. et al., Ilie M. et al. and Longest et al. a turbulence model need to be taken into account when modeling for the continuous phase, even if the aerosol is sprayed into a stagnant or laminar zone [7-11]. This is because of the entrainment of the surrounding fluid, when the droplets are injected, that is so powerful that turbulence is generated locally. When choosing a proper turbulence model for the case of modeling the aerosol spray in the cylinder, the aerosol have been studied visually with an aid of a high speed camera. A rounded plume and tumultuous swirls was witnessed.

Turbulence models that are widely used for simulations of engineering applications are often mathematically based on the Reynolds-decomposition concept. By doing this averaging over time the equations obtained are called Reynolds Averaged Navier-Stokes equations, or simply RANS-equations. When performing the averaging to obtain the RANS-equations an additional term, referred to as the reynold stresses, need to be modeled and closed. This modeling is based on the *Boussinesq approximation* which assumes that the components of the Reynold stress tensor are proportional to the mean velocity gradients of the flow. This approximation further assumes that the turbulence is isotropic, moves in all directions, and that there exist equilibrium between stress and strain [12]. But some inaccuracies stem from the underlying Boussinesq approximation, especially for flows where rapidly strained flows need to be modeled and is not totally isotropic. The turbulence model that have been chosen for this particular case is the two equation model, realizable $k-\varepsilon$. It is due to the fact that this handles rounded plumes and swirls well. The realizable $k-\varepsilon$ model ensures that the normal stresses are positive under all flow conditions, i.e. to ensure realizability, $\langle u_i^2 \rangle \geq 0$. This will make the model perform well for flows involving rotation and separation compared to other $k-\varepsilon$ models, and is well suited flow in which the strain rate is large [12]. Hence, example flows were strain rates are large; plumes and curvatures.

Turbulent dispersion of particles describes how the particles are moving in the fluid due to the turbulence in the continuous phase. One way to model the turbulence dispersion is with discrete random walk (DRW). In DRW the instantaneous velocity is modeled by calculating the mean velocity field and fluctuating velocity component. The fluctuating part (u_i') is modeled using the turbulent kinetic energy (k) and a random number (ξ), see equation (15);

$$u_i' = \xi \sqrt{\frac{2k}{3}} \quad (15)$$

When tracking the particle phase in the continuous phase it is assumed that the particles move between turbulent eddies in the continuous phase. It's modeled that the particle follow the eddy one tenth of the turbulent eddy life time. According to Ilie M et al. and Ruzycki C.A et al. the discrete random walk method produces physically sensible results in many cases when CFD is applied on aerosol modeling [8][10].

3.2.9 Parcels

Using the Eulerian-Lagrangian type of framework makes it easier (if necessary) for FLUENT to bunch a number of particles, who have the same behavior, into a parcel when making calculations. It is assumed that a parcel can be treated in the same way as a particle, i.e. can exchange mass, momentum and heat with the fluid phase. It is also assumed that all particles in a parcel have the same velocity and that there is no void in a parcel (i.e. the parcel density is the same as the material density of the particle).

In this thesis the method chosen in FLUENT to create parcels is called the *standard* method [19]. The number of particles in the parcel is determined as follows;

$$NP = \frac{\Delta t \cdot \dot{m}_s}{m_p} \quad (16)$$

where;

- NP is the number of particles in a parcel
- $\dot{m}_s$ is the mass flow rate of the particle stream
- Δt is the time step
- m_p is the single particle mass

3.2.10 Evaporation

For the case when modeling the spray into the cylinder, calculations have been made to roughly estimate the amount of evaporation that can occur before the system get saturated. These calculations are presented in A.4. The evaporation is estimated for both an adiabatic- and an isothermal case, the isotherm case being the most extreme case. For the adiabatic case, ~4% of the total injected amount of liquid is expected to evaporate until the system is fully saturated. For the isothermal case, ~10% is expected to evaporate. Since small amounts are expected to evaporate in the cylinder, it is assumed that this phenomenon will not make a significant difference when trying to understand the transport of the spray throughout the cylinder. Consequently the evaporation of the droplets will not be taken into consideration.

3.2.11 Droplet deposition on walls

Not much focus was made on the deposition of droplets on the cylinder walls since the main focus was the transport of the droplets. It was simply assumed that when the particles hit the wall, they wet the wall.

4 RESULTS & DISCUSSION

The graphical post processing of the simulations have been done in ANSYS FLUENT. In this section, relevant results are presented followed by analysis and discussion. Some of the results are of experimental nature and it will be made clear when these are presented.

4.1 Flow field in IDA-geometry

It was determined in section 3.1 that the flow regime of the continuous phase in IDA is laminar due to the low bulk Reynolds numbers of about 14. Figure 9 shows a contour plot of the cell Reynolds numbers obtained when simulating the flow through the device. The cell Reynolds number is based on the velocity in the calculation cell and the (cell volume)$^{1/3}$. It is interpreted that the highest cell Reynolds numbers are in the inlet pipe and as the flow is transported into the closed exposure chamber the cell Reynolds number is decreased, just like we expected it to do when examining this matter under section 3.1. It can also be observed that the highest cell Reynolds numbers in the system are well below 2100 and it is therefore justified that the flow is laminar when only air is flowing through the system.

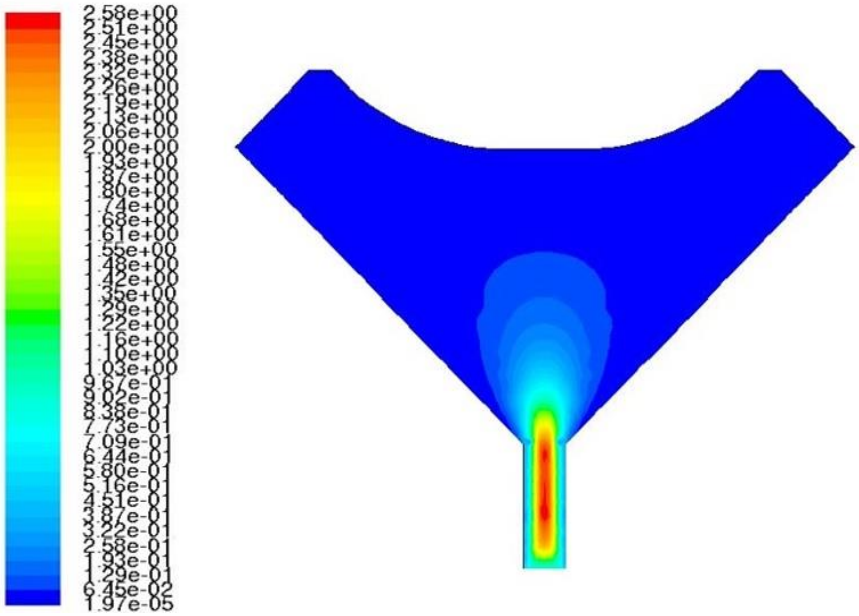

Figure 9. Contour plot of cell Reynolds number in IDA.

It is also seen in Figure 9 that the cell Reynolds number is highest in the center of the inlet pipe and gradually decreased as getting closer to the wall, this is due to the parabolic velocity profile mentioned earlier. By looking really closely in Figure 9 it can also be seen that it takes a certain length for this parabolic profile to develop, earlier we called this the entrance length, and it was determined to be about 10mm. Figure 10 illustrates plots for different entrance lengths in the inlet pipe. The data for these plots where obtained from the simulation. By studying this plot it can be seen that a parabolic velocity profile is developing as longer into the pipe the flow gets and after about 10-13mm the velocity profile is almost identical. That concludes that it takes about 10-13mm to develop a parabolic velocity profile. This justifies our hand-calculated entrance length and it also validate that the inlet pipe, of 30mm, is long enough to obtain a fully developed flow.

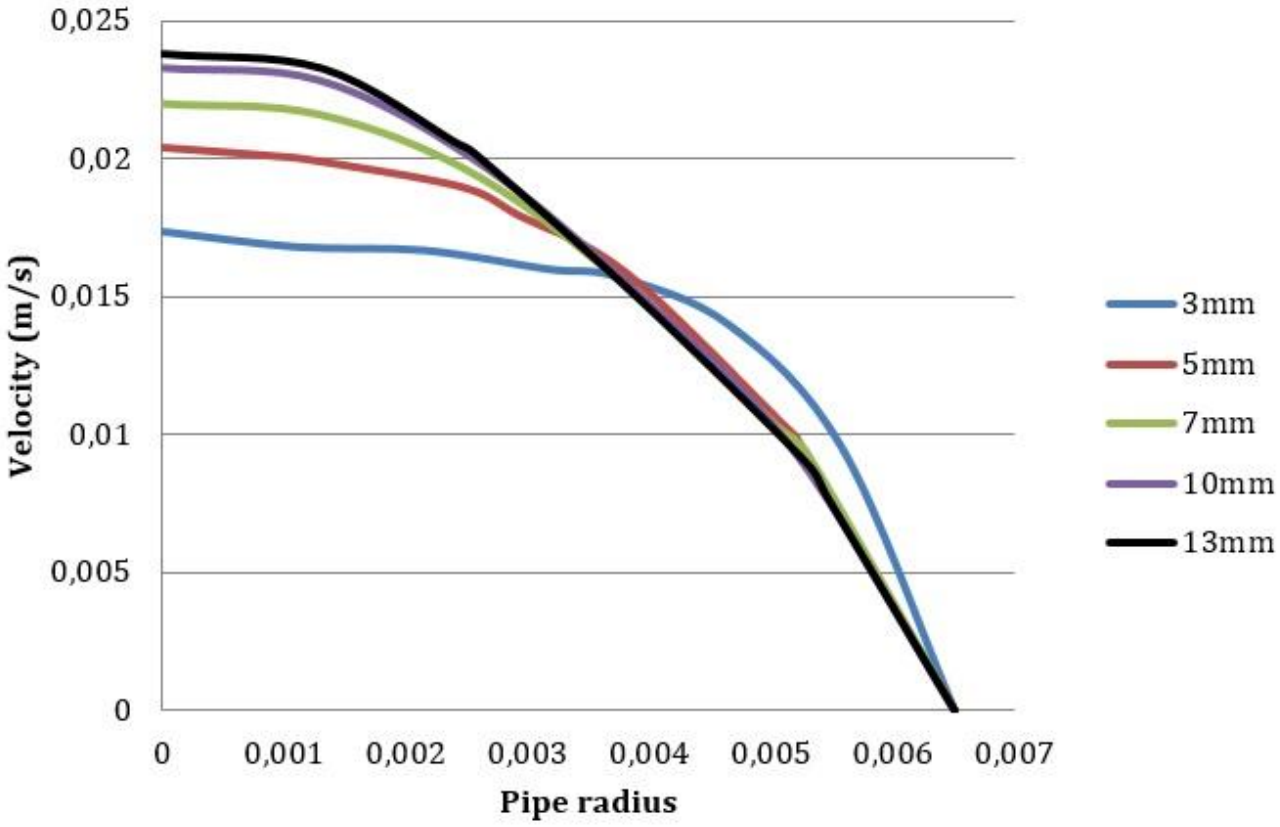

Figure 10. Velocity profiles in the inlet pipe.

4.2 Droplet flow in the cylinder geometry

In section 3.2.1, it was explained that CFD simulations was made concurrently with experimental analysis. It was also mentioned that an iterative process have been performed to try to match the CFD results with the experimental results as well as possible. 1000µL/min of water was sprayed into the cylinder for both the CFD- and experimental case.

4.2.1 Physics

First and foremost, results that provide us with information and understanding about the physics around the nebulizer will be presented. In Figure 11a, the plume of the aerosol spray that has been developed after 0.09 seconds can be seen. As was explained in section 3.2.6, this spray is expected to entrain the surrounding air and the direct result of this phenomenon is presented in Figure 11b.

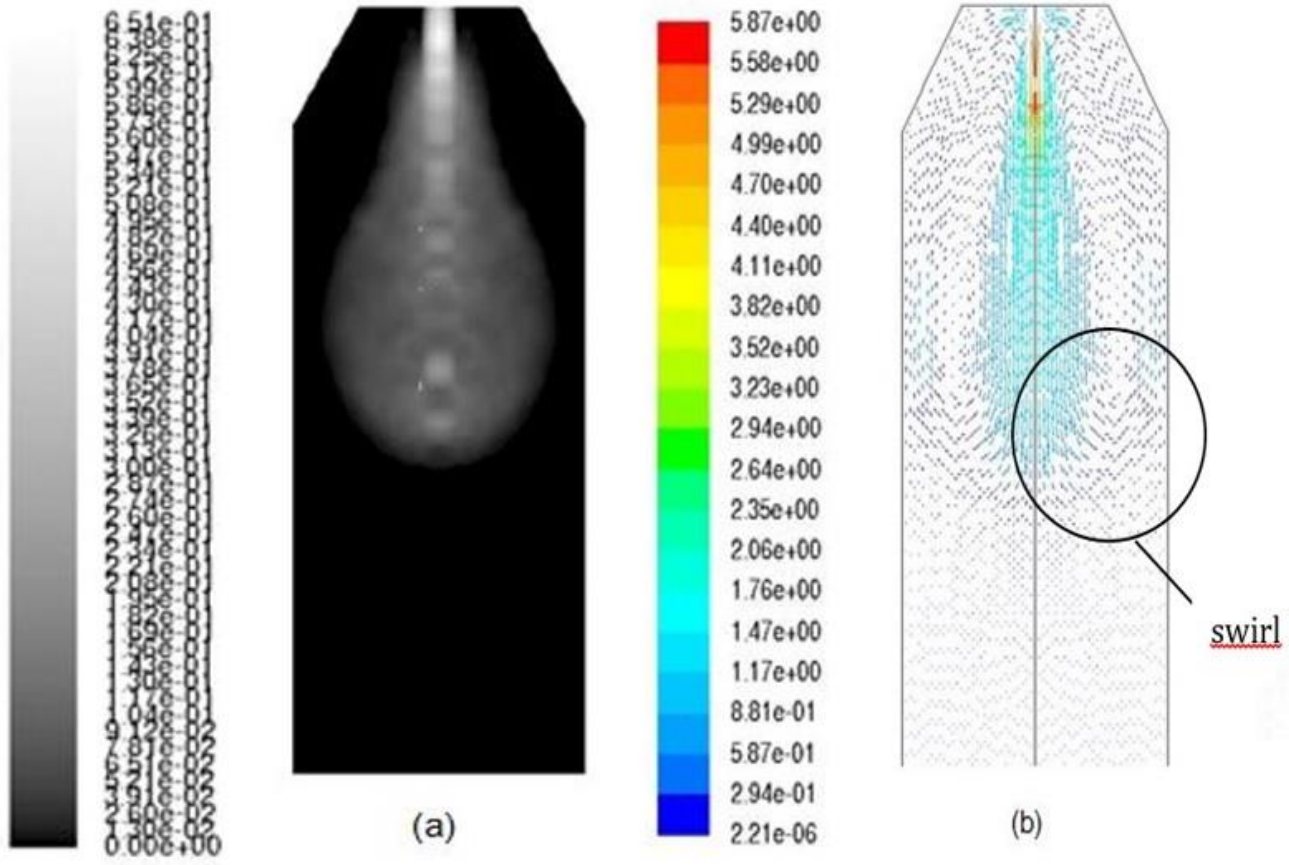

Figure 11. (a) Concentration (kg/m³) of dispersed phase in cylinder. (b) velocity vectors of air

The largest velocity gradients of the air are streaming downwards in the cylinder due to the aerosol being injected downwards. By looking closely in Figure 11b some swirls can be witnessed as well. As was mentioned in section 3.2.8, curvatures in the aerosol cloud can be seen when studying the experimental case with the high speed camera and the swirls seen in Figure 11b is believed to be the direct reason for those swirls. Figure 12 below is a zoomed in illustration of the area in the cylinder were curvature and swirls of the air can be seen. Since the Stokes number is expected to be well below unity, many droplets follow the swirls of the air and is therefore visible in the experimental case. These swirls are believed to be one of the reasons, among others, the aerosol is spread over the whole cylinder domain.

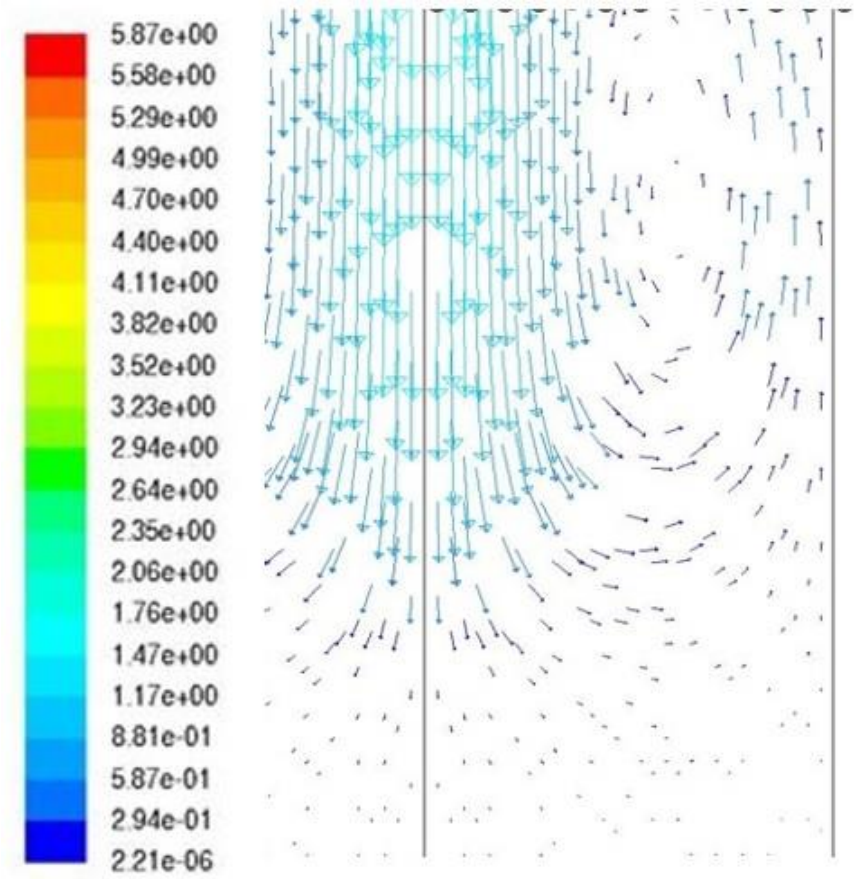

Figure 12 . Illustration of swirls in the continuous phase in the cylinder.

This entrainment of the surrounding fluid is so powerful (heavy coupled) that turbulence is generated locally. In Figure 13, the turbulent kinetic energy (k) is presented. Keep in mind that the fluid was stagnant (initial value for kinetic energy: $1 \cdot 10^{-8}$ m^2/s^2) prior to spraying the dispersed phase into the cylinder. It can be noted that at the inlet where the spray is most dense and the two phases are the most heavily coupled, is where the turbulence is the mostly generated.

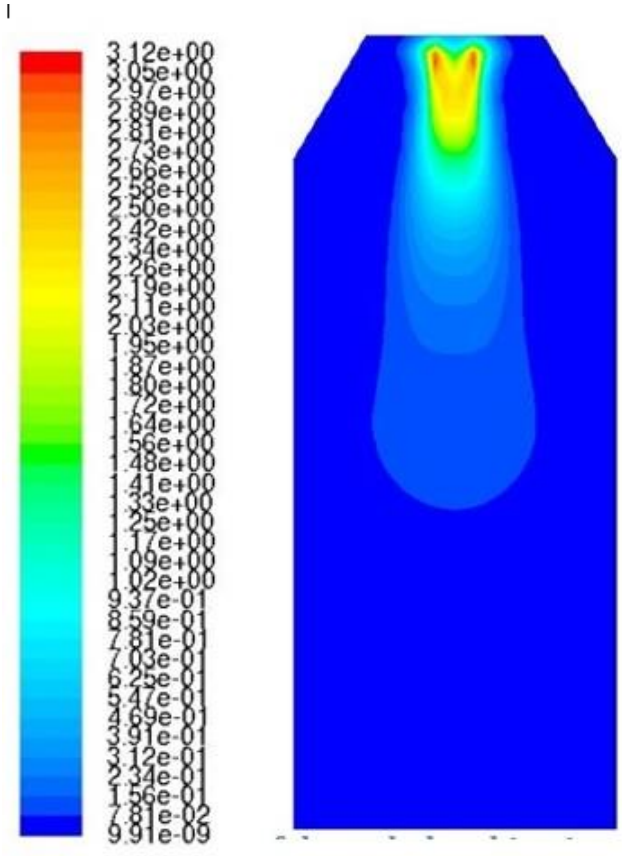

Figure 13. Contour plot of the turbulent kinetic energy (k) in the cylinder.

4.2.2 CFD- vs. experimental case

CFD-simulations was validated by comparing them to the in vitro results obtained by the high speed camera. The dispersed phase was given an initial velocity of 20 m/s when modeled in FLUENT. In this section, only an arbitrary case of the results will be presented. More results can be found in A.5. Figure 14a illustrates a snapshot of the simulation after 0.18 seconds. This snapshot is compared with a snapshot from the experimental case, see Figure 14b, which is also taken after about 0.18 seconds of spraying into the cylinder. It can be witnessed that the aerosol have been transported approximately equal distance for both cases and that the spread in the cylinder domain is similar as well. This gives an indication that the modeling of the dispersed phase injected into the cylinder with an initial velocity of 20 m/s might describe the system quite well. Through further analysis with the high speed camera, velocity fluctuations of the incoming spray was witnessed to be around 1 m/s. It can be seen that the k-value in figure 13 is ~ 2 where the turbulence is generated and that is equivalent to fluctuations of ~ 1 m/s. The velocity fluctuation u_i' being $\sim \sqrt{k}$. Thus, that being a validation that the CFD-simulations agree with what is seen in the experimental case. However it is essential to keep in mind that this direct comparison with a visual interpretation is a qualitative analysis and cannot be generalized with other cases. But it can be a good source for a hypothesis where its general validity can be tested and verified with quantitative methods and analysis. Consequently these results are preliminary and give a more general idea of the system.

When looking upon the results presented in Figures 14a and 14b and comparing these, a valid discussion can be made about what aerosol concentration that can be seen with the naked eye. For instance, in Figure 14a it can be seen that the lowest aerosol concentration that is perceived as an existing aerosol cloud have a concentration of about 12 grams/m^3. A crucial question to ask oneself is if this concentration of the dispersed phase is visible to the naked eye. That is obviously something that is very difficult to determine

without any analytical tool since this depends on several parameters. The lightning and the distance from the aerosol cloud is important parameters, among others, that determine if the cloud can be witnessed for instance. Quantitative analysis where measurements of the aerosol cloud, for the experimental case, can be of central interest to determine what the concentration actually is in the cylinder. If that is known, a more truthful comparison between the CFD-simulation and the experimental case can be made.

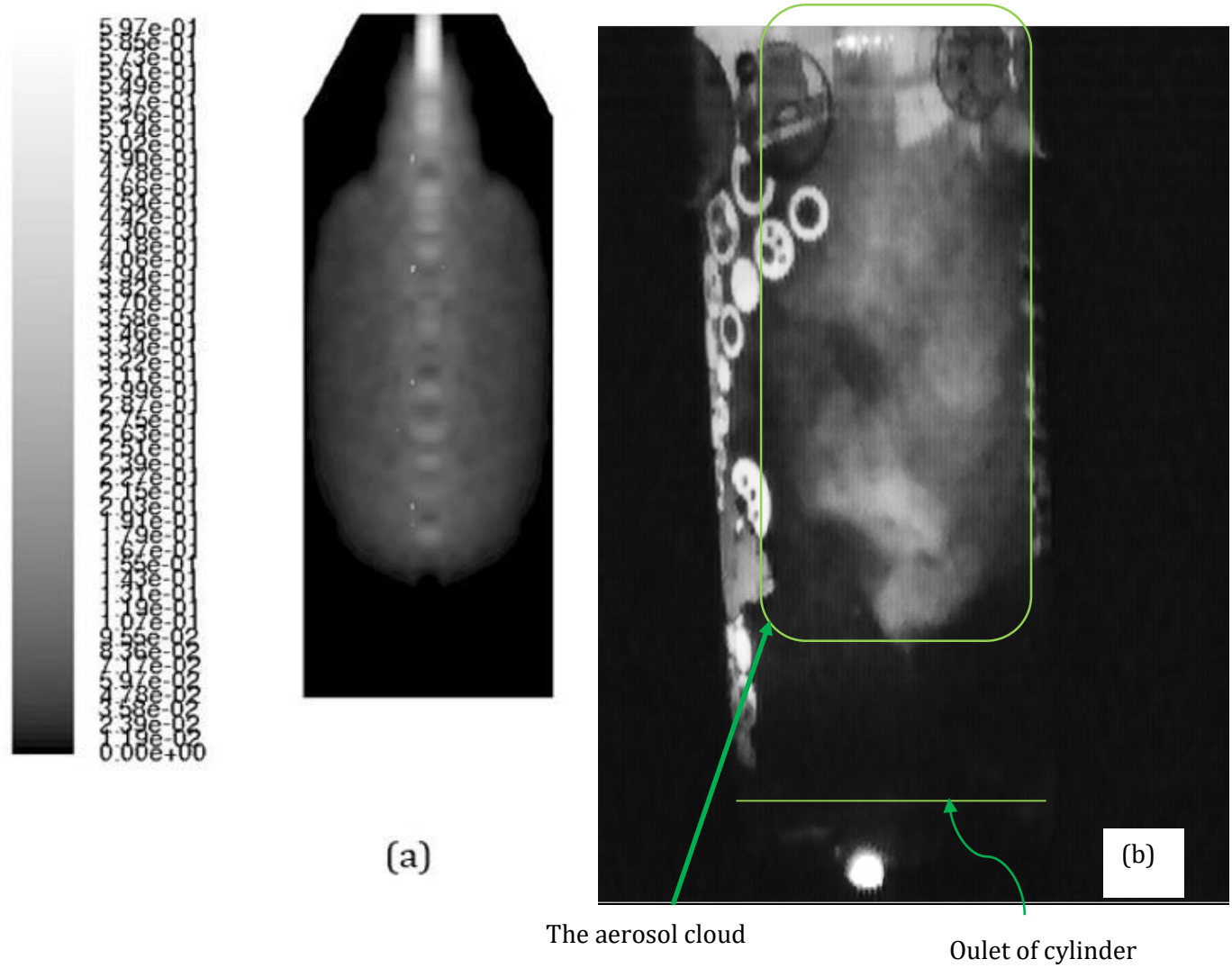

Figure 14. After 0.18 seconds. CFD simulation to the left and snapshot with high speed camera to the right.

Additional figures where the CFD-simulations and experiments are compared can be seen in A.5. The aerosol development in the cylinder over several time steps is also presented in A.6. For the latter time steps when the substance have been sprayed into the system for more than about 1.6 seconds, see Figure 27 in A.6, a gradual increase of the aerosol concentration can be seen. A build up of the aerosol concentration in the cylinder is expected until it eventually reaches steady state, i.e. the amount of substance sprayed into the cylinder is equivalent to the amount exiting the system. However, simulations where not made for that amount of times till steady state was reached. That was because of too many

particles being present after about 2.5 seconds and the simulations ended up being too computationally expensive. Yet, the gradual build up of the aerosol concentration can be noted in the cylinder and is presented in Figure 15.

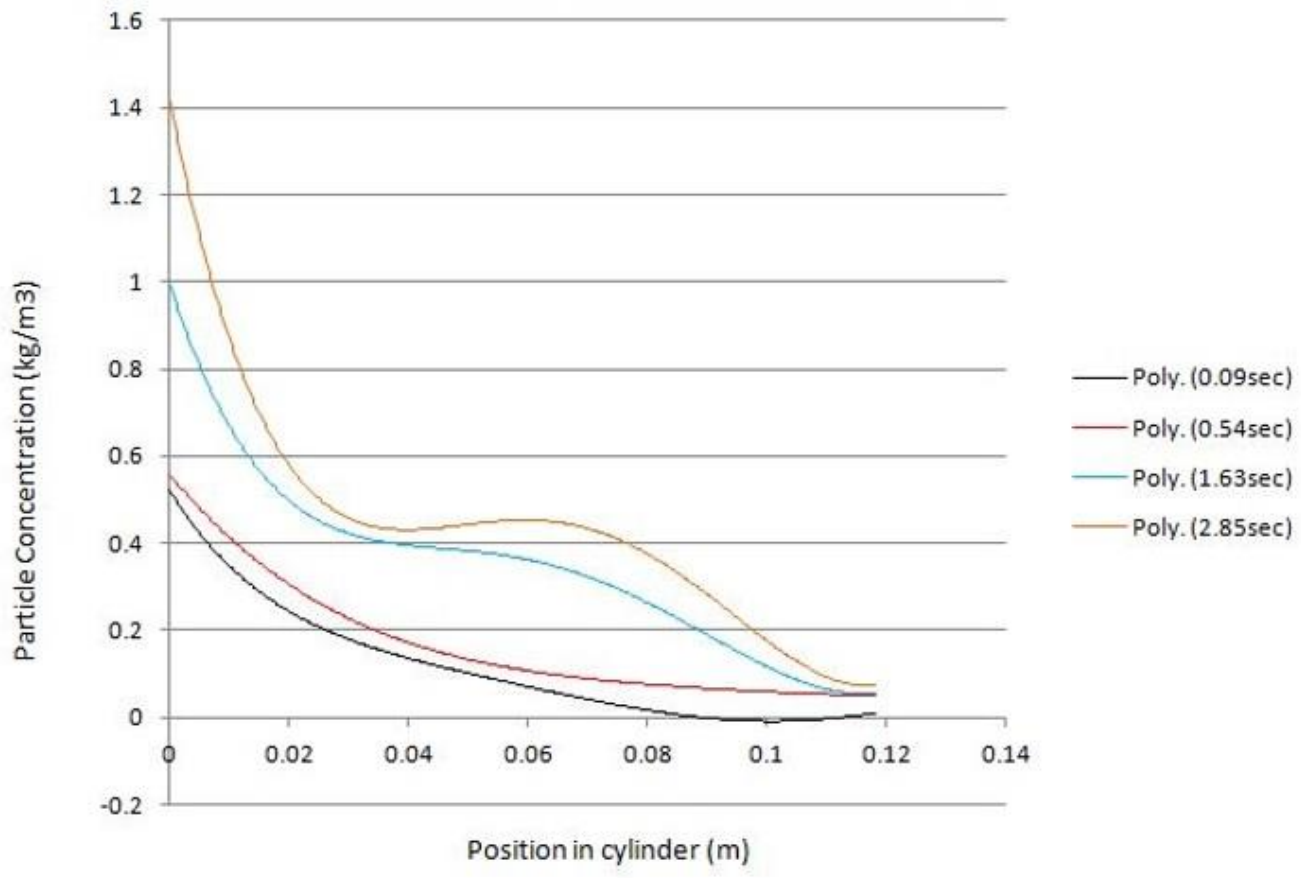

Figure 15. Aerosol concentration along the symmetry axis in the cylinder. The curves are for specific times.

4.3 Introducing droplets in the IDA-geometry

When modeling a nebulization of 1000µL/min, an inlet velocity of 20 m/s was determined to best match the in vitro results for the cylinder. In this section, results will be presented when substance is sprayed into the IDA geometry but with the exact same modeling parameters as for the cylinder. Keep in mind that this was done although there is considerable uncertainty, and the results that are eventually obtained will mainly determine if the modeling and understanding of the nebulizer and the system is on the right track. Figure 16 is an illustration of the dispersed phase concentration in IDA when substance has been sprayed for 2.6 seconds.

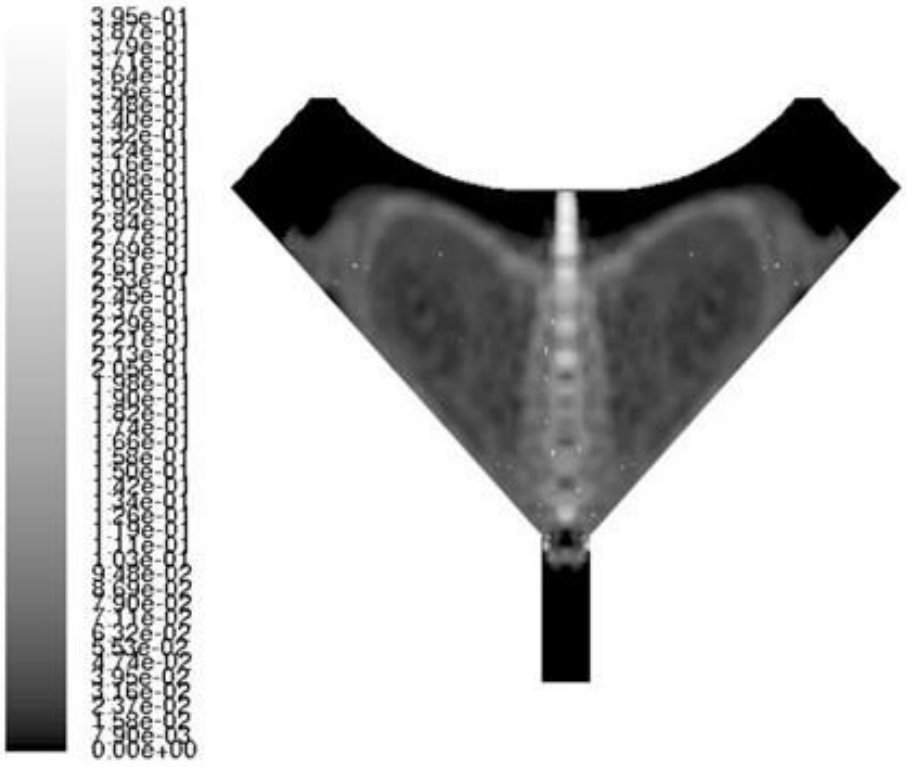

Figure 16. Concentration of the dispersed phase in IDA after 2.6 seconds of nebulization.

The main way of going about validating the results obtained in Figure 16 for this thesis is through experience of the system and very simple qualitative analysis. First of all, getting a spread of the aerosol in the whole volume of the closed exposure chamber is promising and can easily be validated by just looking into the closed exposure chamber with the naked eye. But keep in mind that yet remains the discussion and uncertainty of what aerosol concentration that can be seen with the naked eye, which was discussed earlier. Another aspect that is interesting to study for a rough validation, is to look at the time it takes to fill up the closed exposure chamber and determine when the aerosol cloud can be seen, with the naked eye, exiting the rodent outlets. In Figure 16, the system have been simulated for 2.6 seconds and that is approximately the amount of time it takes for the aerosol cloud to reach the rodent outlets. See A.7 to get a more clear idea about how the aerosol cloud is spread over the closed exposure chamber over time.

When 1000µL/min is aerosolized into IDA experimentally, for the reason to try to determine for what time the aerosol cloud can be seen exiting the rodent outlet, it takes approximately 2-4 seconds until the substance can be seen coming out the outlet. This indicates that the dispersed phase is around the rodent outlet for approximately the same time range for both the CFD- and experimental case. Figure 17 below is a picture of how it might look like when an aerosol cloud is exiting the rodent outlet.

Figure 17. Aerosol cloud (looking like smoke) exiting the rodent outlet.

5 CONCLUSIONS

A novel design of a rodent nose-only inhalation device for animals has been studied. A CAD-model of the device was designed which give a converging system and it could be determined that the flow through the device, when no dispersed phase is involved, is laminar.

The main focus have been to understand the physics of the system and the understanding of the vibrating mesh nebulizer since not much information is provided about this unit by the manufacturer. It has been concluded that the dispersed phase, injected from the nebulizer, entrains surrounding air resulting in an induced flow that propels the droplet beyond their individual stopping distance i.e. the dispersed phase and the continuous phase are two-way momentum coupled, since the characteristic measure of phase coupling, π_{mom}, is confirmed to be high close to the nebulizer. The entrainment of the surrounding fluid is to the extent that turbulence is generated and therefore a turbulence model is needed when modeling the continuous phase when a dispersed phase is involved, this will more or less give truthful results when comparing to the real case scenario.

When the nebulizer has been studied, 1000µL/min has been the amount of liquid sprayed into a cylinder. The CFD results have been compared with the experimental in vitro results, obtained with a high speed camera, and a hypothesis have been confirmed that a inlet velocity of about 20 m/s should be set for the dispersed phase, when injected into the cylinder, for the CFD results to match the in vitro results. Through further analysis with the high speed camera velocity fluctuations of the incoming aerosol cloud was witnessed to be around 1 m/s, which matches well with the k-values obtained from the simulations. This gives information that the simulations agree well with in vitro results. The inlet velocity of 20 m/s, when 1000 µL/min is injected, is humbly called a hypothesis since it is not yet concluded if the CFD results can be directly compared with the in vitro results since it's not concluded what aerosol concentration that can be seen with the naked eye.

6 POTENTIALS FOR FUTURE WORK

It has been concluded that a turbulence model should be taken into account when the dispersed phase is injected into the system. The turbulence model chosen in this thesis was $k-\varepsilon$ realizable. This turbulence model was mainly chosen by studying the flow characteristics that was obtained with the high speed camera. It could be seen that a rounded plume and swirls were present and a $k-\varepsilon$ realizable was chosen due to the fact that it can handle those kinds of flow characteristics. However, when the results have been obtained it has been realized that that the turbulence is present but it is mainly low turbulence (Re<50 000) [12]. The flow is even laminar in some areas. Therefore a turbulence model like $k-\omega$ can be of high interest since it performs well for low turbulence. For future work the $k-\omega$ turbulence model should also be tried out to see if better results are achieved.

It has frequently been discussed in this thesis that the results obtained by the CFD-simulations cannot be directly compared with the in vitro results since it is not known what aerosol concentration that can be seen with the naked eye. For further work, it is suggested that some kind of measurement is made to give information about what the aerosol mass concentration is in the in vitro case so it can be compared with simulations for just validations. Szymanski W.W suggest that a laser aerosol spectrometer (PMS-LAS-X) can be used to determine the particle number concentration, and since the particle mass is known the mass concentration can be calculated. The more interested reader is referred to [20] for more detailed information.

In this thesis, many of the conclusions drawn and information obtained is for the case when 1000µL/min is injected from the nebulizer. This is because 1000µL/min is easily injected by hand so quick and simple in vitro trials are made. However, when rodents are dosed with newly developed substances ~20µL/min is sprayed into the closed exposure chamber. Consequently further work remains to understand the physics and boundary conditions for the nebulizer when 20µL/min is injected. With this thesis as a pre-study, building up an understanding of the system when 20µL/min is injected is believed to be achieved rather quickly.

Keep in mind that the cases presented above should be made for the simple cylinder geometry. When these are achieved one can start thinking about going over to the 2D axi-symmetric geometry of IDA. The evaporation of the droplets should eventually be taken into account as well when doing the simulations in the IDA geometry. That is because the evaporation of the droplets is expected to be crucial for the classification of droplets in the closed exposure chamber. Finally the breathing pattern of the rodents can be set as boundary conditions at the rodent outlets to observe what kind of impact that has on the system.

Although effects of the two-way momentum coupling between the aerosol spray and the gas phase are significant, simulating this interaction is numerically very expensive and limits the extent of the study. Therefore studying an alternative way to model the system might be worthwhile since it might make the simulations much less computationally expensive. This alternative way is suggested by Longest P.W et al. and it suggests that a small air flow should be injected concurrently with the dispersed phase [7]. This small air jet will approximate the aerosol impact on the gas phase in a one-way coupled simulation. This alternative way of modeling the system can potentially give the same physics in the system, as the two-way coupled case, whilst the heavy two-way momentum coupling is not present and the simulations are less expensive.

7 NOMENCLATURE

A_{sphere}	Area of sphere (m^2)
C_D	Drag coefficient
d	characteristic diameter (m)
d_p	particle diameter (m)
D	inne diameter of pipe (m)
g	gravitation (m/s^2)
k	turbulent kinetic energy (m^2/s^2)
L_e	Entrance length (m)
m	mass (kg)
m_p	particle mass (kg)
$\dot{m}_p$	mass flow rate of particle stream (kg/s)
n_{pj}	unit normal vector
NP	number of particles in a parcel
∇p_f	pressure gradient in fluid phase
Re	Reynolds number
Re_p	Particle Reynolds number
S_{mass}	mass source term (kg/m^3s)
S_p	momentum source term (N/kg)
St	Stokes number
Δt	time step (s)
u	velocity (m/s)
u_f	velocity of fluid phase (m/s)
u_p	velocity of dispersed phase (m/s)
u'_i	fluctuating velocity (m/s)
V	Volume (m^3)
V^i	volume occupied by dispersed phase (m^3)
ν	kinematic viscosity (m^2/s)
α_d	volume fraction of dispersed phase
α_f	volume fraction of fluid phase
ρ_f	density of fluid phase (kg/m^3)
ρ_p	density of dispersed phase (kg/m^3)

τ_f	fluid flow time scale (s)
τ_{xp}	particle relaxation time (s)
μ_f	dynamic viscosity of fluid (Pas)
σ_{fij}	shear stress (Pa)
$\bar{\rho}_d$	Apparent density of dispersed phase
$\bar{\rho}_c$	Apparent density of continuous phase
Π_{mom}	Phase coupling characteristic

8 REFERENCES

[1] – Sandeau J. Katz I. Fodil R. Louis B. Apiou-Sbirlea G. Caillibotte G. Isabey D., CFD simulations of particle deposition in a reconstructed human oral extrathoracic airway for air and helium-oxygen mixtures, Journal of Aerosol Science 41, p.281-294, 2010.

[2] –Zhang Z. Kleinstreuer C. Kim C.S., Comparison of analytical and CFD models with regard to micron particle deposition in a human 16-generation tracheobronical airway model, Aerosol Science 40, p.16-28, 2009.

[3] –Cryan S. Sivadas N. Garcia-Contreras L., In vivo animal models for drug delivery across the lung mucosal barrier, Advanded Drug Delivery Reviews 59, p.1133-1151, 2007.

[4] – Wu Y. Kotzer CJ. Makrogiannis S. Logan GA. Haley H. Barnette MS. Sarkar SK., A Noninvasive [^{99m}Tc]DTP ASPECT/CT Imaging methodology as a measure of lung permeability in a guinea pig model of COPD, Academy of Molecular imaging and society for molecular imaging, 14 September 2010.

[5] – http://www.aerogen.com/technology/vibronic.html, Vibtronic™, How does it work?, Accessed 4 May 2015.

[6] – Lee, S.H., Nano spray drying: A novel method for preparing protein nanoparticles for protein therapy, International Journal of Pharmaceutics, volume 403, Issues 1-2: p.192-200, 17 January 2011.

[7] – Longest, P.W and Hindle, M, Evaluation of the Respimat Soft Mist Inhaler using a concurrent CFD and in vitro approach, Journal of aerosol medicine and pulmonary drug delivery, volume 22, number 2, pp. 99-112, 2009.

[8] – Ruzycki, C.A Javaheri E. Finlay W.H., The use of computational fluid dynamics in inhaler design, Expert Opinion, University of Alberta, 2013.

[9] - Wong W. Fletcher D. Traini D. Chan H. Young P., The use of computational approaches in inhaler development, Advanced Drug Delivery Reviews 64, p. 312-322, 2012.

[10] – Ilie M. Matida E.A. Finlay W.H., Asymmetrical Aerosol Deposition in an idealized mouth with a DPI mouthpiece inlet, Aerosol science and technology 42, p. 10-17, 2008.

[11] – Longest P.W Hindle M. Choudhuri S. Byron P., Numerical simulations of capillary aerosol generation: CFD model development and comparisons with experimental data, Aerosol science and technology 41, p. 952-973, 2007.

[12] – Andersson B. Andersson R. Håkansson L. Mortensen M. Sudiyo R. van Wachem B., Computational Fluid Dynamics for Engineers, Cambridge University Press, 2011.

[13] – Welty JR et al., Fundamentals of Momentum, heat, and mass transfer, 5th edition, John Wiley & Sons Inc., 2007.

[14] – Durst F. Milojevic D. Schönung B., Eulerian and Lagrangian predictions of particulate two-phase flows: a numerical study, Appl. Math. Modelling, Vol. 8, April 1984.

[15] – Sasic Srdjan, Multiphase Flows Course, Lecture 4, slide 71, 2014.

[16] – Sommerfeld M. Van Wachem B. Oliemans R., ERCOFTAC Special Interest Group on ”Dispersed turbulent multi-phase flow”, October 2007.

[17] – Sasic Srdjan, Multiphase Flows Course, Lecture 2, slide 17, 2014.

[18] - Eslamian M. Ashgriz N., Effect of Atomization Method on Morphology of Spray-Generated Particels, Journal of Engineering Materials and Technology, Vol. 129, January 2007.

[19] – ANSYS Theory Guide, ANSYS Inc, 2013.

[20] – Szymanski W.W, Aerosol concentration measurement with multiple light scattering system and laser aerosol spectrometer, Atmospheric Research, Volume 62, Issues 3-4, p. 255-265, June 2002.

[21] – Mörtstedt S.E Hellsten G., Data och Diagram Energi- och kemitekniska tabeller, Liber, 2010.

9 APPENDIX

A.1 Volume fraction of dispersed phase

When examining the spray injection in the cylinder, 1000 µliter/min of substance is injected. That is equivalent to $1 \cdot 10^{-6}\ m^3/min$ ($\dot{V}$ substance).

Average cell dimension is about 0.001 m in the injection area. The velocity of the dispersed phase is estimated to be 2 m/s just after the substance have been injected into the cylinder, keep in mind that this is an underestimation for ultimately calculating a volume fraction in a extreme case scenario.

The average residence time over the cell is then;

$$\tau = \frac{0.001\ m}{2\ m/s} = 5 \cdot 10^{-4}\ s$$

--> $5 \cdot 10^{-4}\ s\ \times 1.67 \cdot 10^{-8}\ {}^{m^3}/_{s} = 8.35 \cdot 10^{-12} m^3$ substance in the cell.

Total volume of the cell is $1 \cdot 10^{-9}\ m^3$.

$$\frac{8.35 \cdot 10^{-12}}{1 \cdot 10^{-9}} = 8 \cdot 10^{-3}\ (volume\ fraction\ dispersed\ phase)$$

A.2 Calculation of τ_{xp}

$$\tau_{xp} = \frac{\rho_p d_p^2}{18\mu_f} \quad (17)$$

$\rho_p \sim \frac{1000kg}{m3}$

$d_p \sim average\ 5\mu m$

$\mu_f(dynamic\ viscosity\ for\ air) = 18.2 \cdot 10^{-6}\ Pas$ [21]

➔ $\tau_{xp} = 7.6 \cdot 10^{-5}\ seconds$

A.3 Numerical solution for equation of motion

Final expression to be solved when drag force and gravitational force is taken into account;

$$\frac{du_p}{dt} = g - \frac{3}{4}\frac{\rho_f}{\rho_p}\frac{24}{Re_p}\frac{1}{d}(u_p)^2 \quad (18)$$

Numerical solutions for the differential equation;

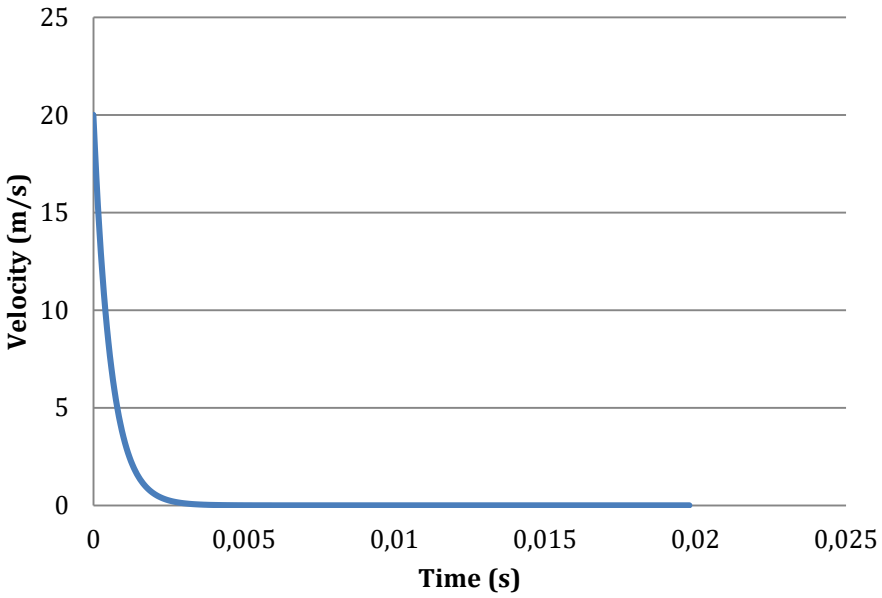

Figure 18. Velocity for an individual particle.

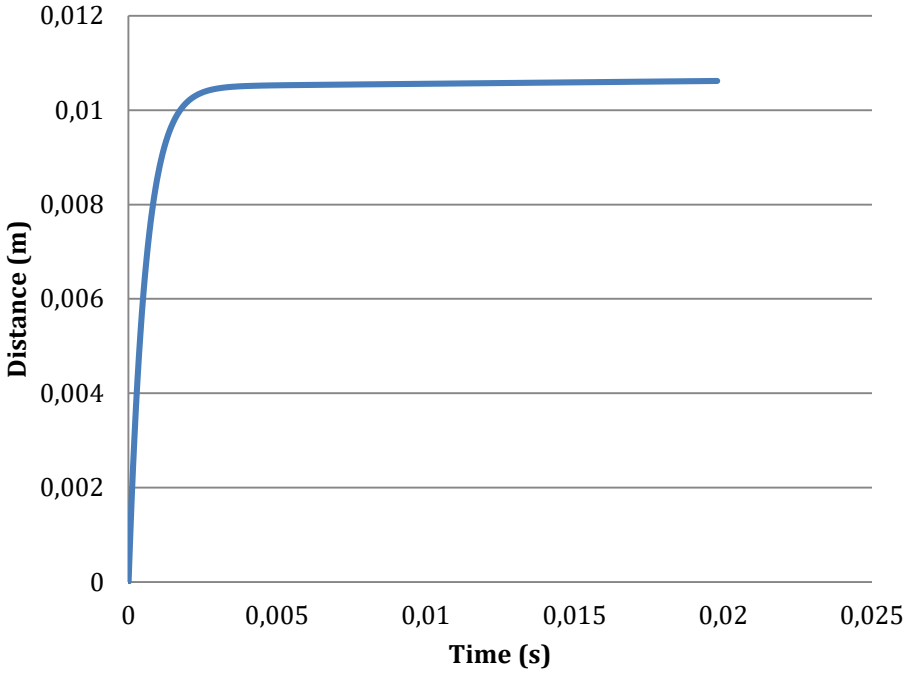

Figure 19. Distance for an individual particle.

Figure 19 shows that the particle travels a very short distance before it's decelerated to its terminal velocity. The terminal velocity can be obtained from Figure 19 by calculating the slope of the linear part of the curve.

The terminal velocity obtained is $6 \cdot 10^{-3} \frac{m}{s}$.

A.4 Evaporation of droplets

This is a rough estimate for the evaporation of the droplets in the cylinder.

1000µL/min is sprayed into the system.

1000µL/min --> $1000 \cdot 10^{-6} kg/min$ --> $1.66 \cdot 10^{-5}\ kg/s$

$1.66 \cdot 10^{-5}\ kg/s$ water is sprayed into the system.

The total volume of the cylinder is $1.2566 \cdot 10^{-4}\ m^3$ and when assuming the density of air being $\sim 1\ kg/m^3$ --> $1.2566 \cdot 10^{-4}\ kg$ (is the mass of air in the cylinder)

Adiabatic case

0.0058 kg H_2O/ kg dry air <-- can be picked up until the air gets saturated [21]

For $1.2566 \cdot 10^{-4}$ kg dry air, $7.28 \cdot 10^{-7}$ kg H_2O can be picked up. Keep in mind that this if for a case when the air is initially totally dry. This is OK since we want to do the calculations for extreme cases.

$\frac{7.28 \cdot 10^{-7}}{1.66 \cdot 10^{-5}} = \sim 4\%$ --> 4% of what you inject during 1 second will evaporate.

Isothermal case

0.014 kg H_2O/ kg dry air <-- can be picked up until it gets saturated [21]

$1.76 \cdot 10^{-6}$ kg H_2O can be picked up.

$\frac{1.76 \cdot 10^{-6}}{1.66 \cdot 10^{-5}} = \sim 10\%$ --> 10% evaporate during 1 second.

A.5 CFD- vs. experimental case

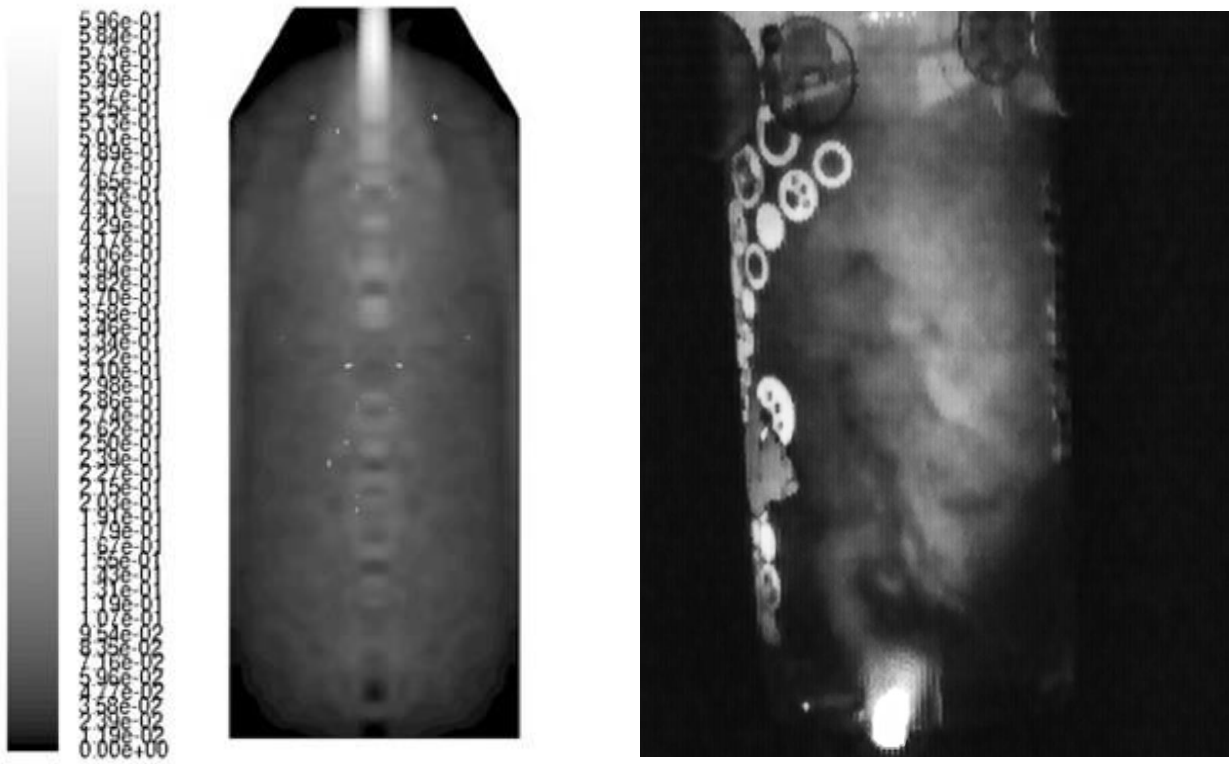

Figure 20. After 0.36 seconds. CFD simulation to the left and snapshot with high speed camera to the right.

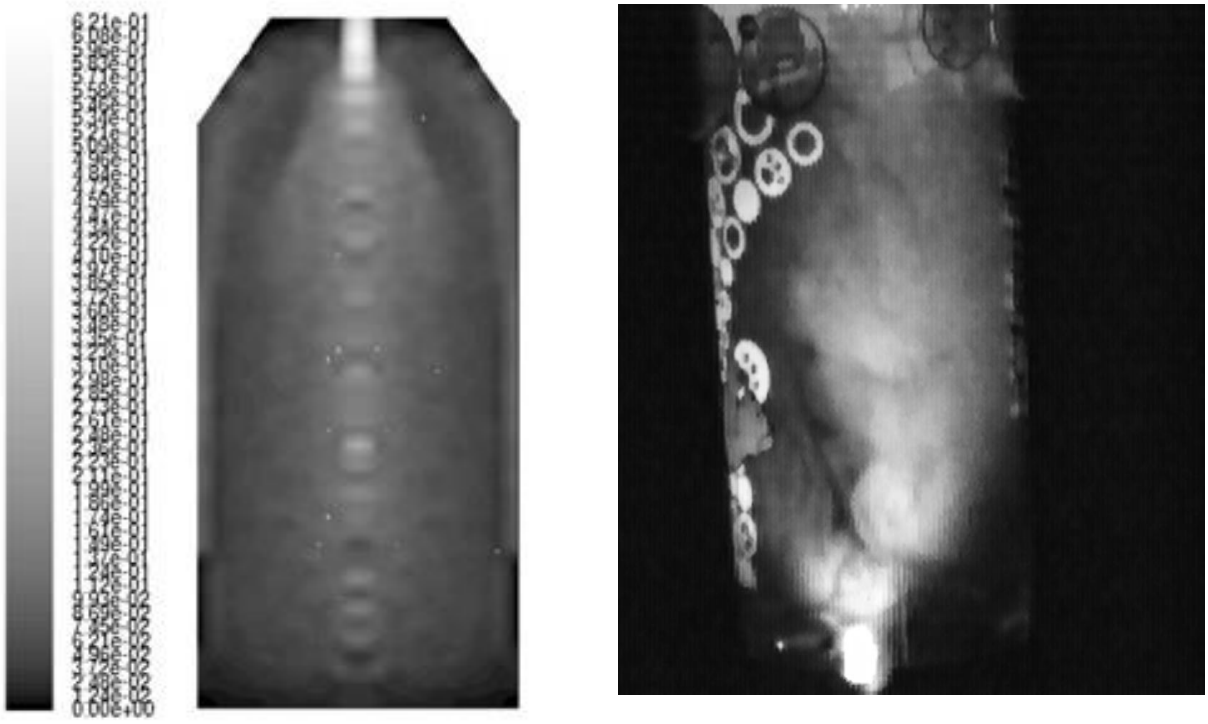

Figure 21. After 0.54 seconds. CFD simulation to the left and snapshot with high speed camera to the right.

A.6 Aerosol cloud in cylinder for different times

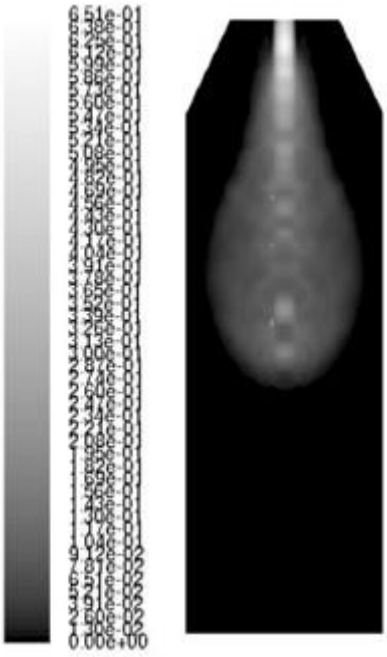

Figure 22. 0.09 seconds

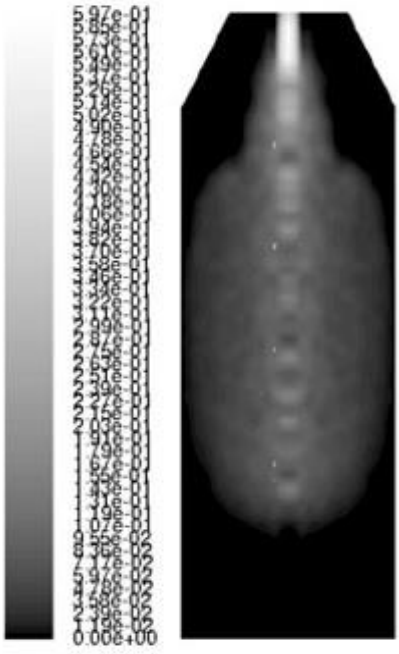

Figure 23. 0.18 seconds

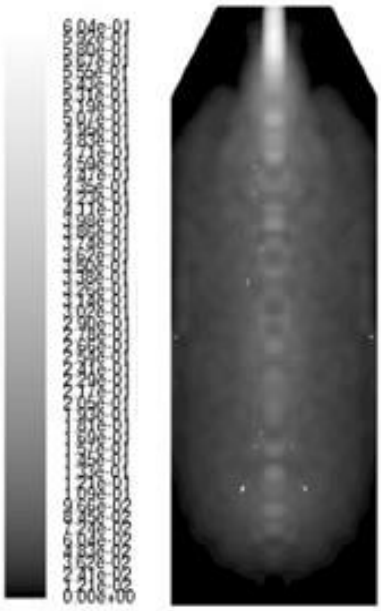

Figure 24. 0.27 seconds

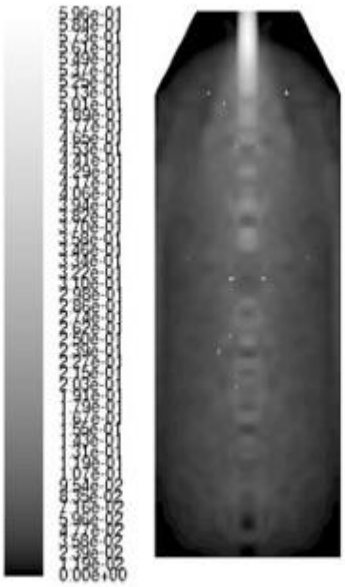

Figure 25. 0.36 seconds

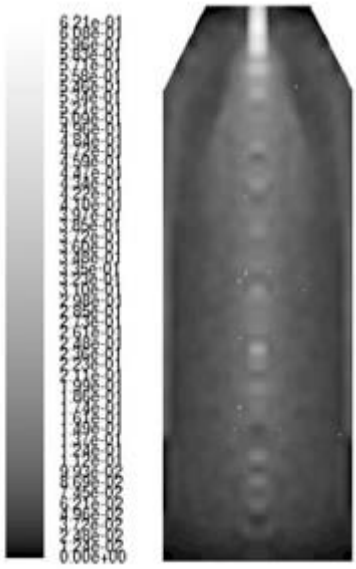

Figure 26. 0.54 seconds

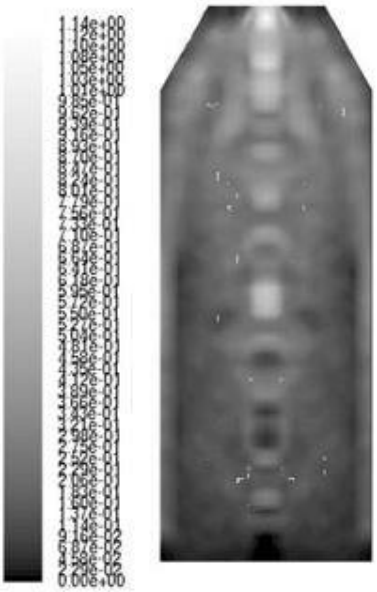

Figure 27. 1.63 seconds

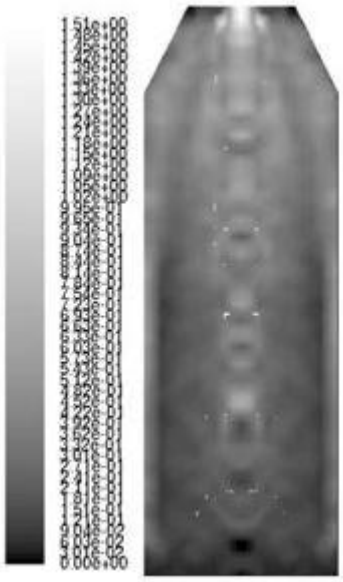

Figure 28. 2.85 seconds

A.7 Dispersed phase in IDA for different times

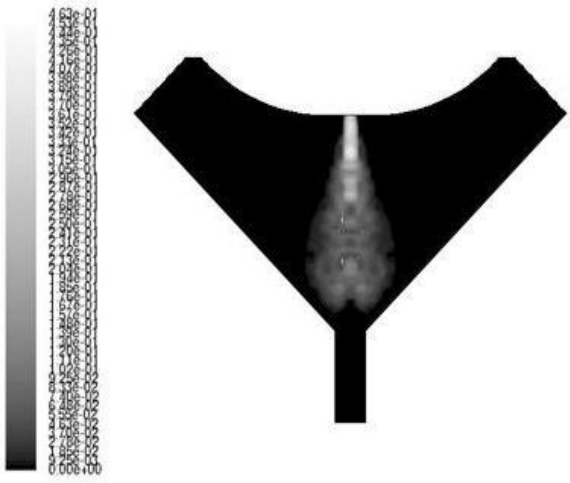

Figure 29. 0.1 seconds

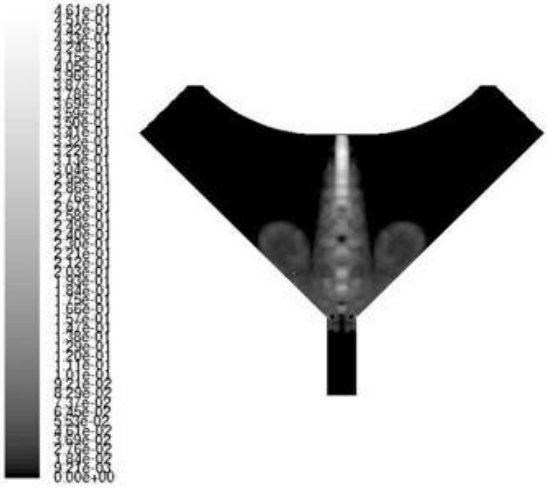

Figure 30. 0.3 seconds

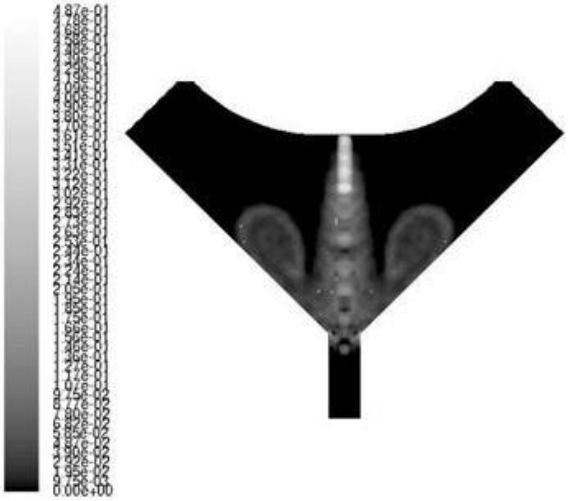

Figure 31. 0.5 seconds

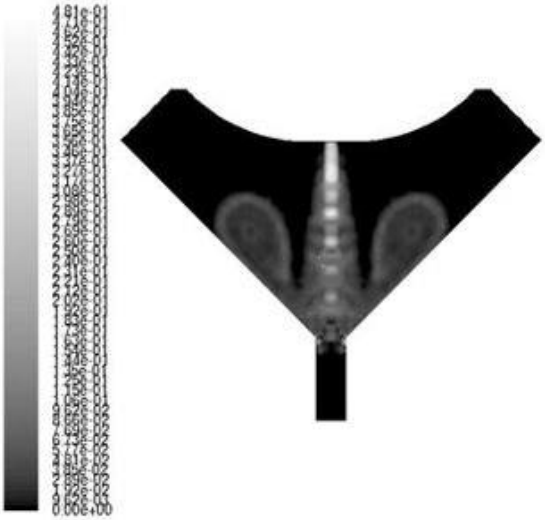

Figure 32. 0.7 seconds

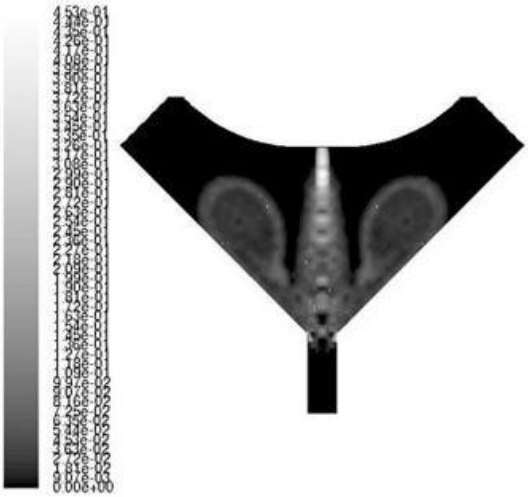

Figure 33. 1.0 seconds

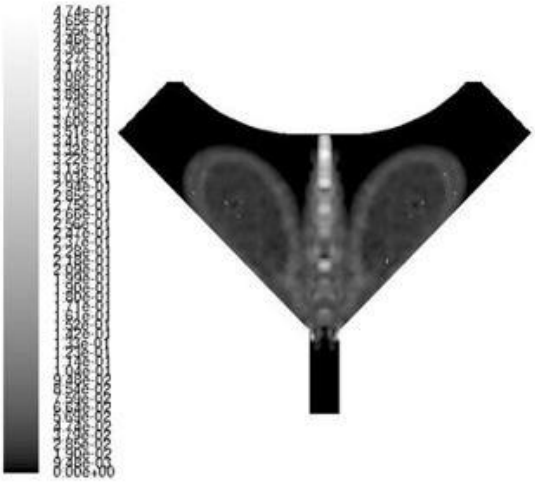

Figure 34. 1.5 seconds

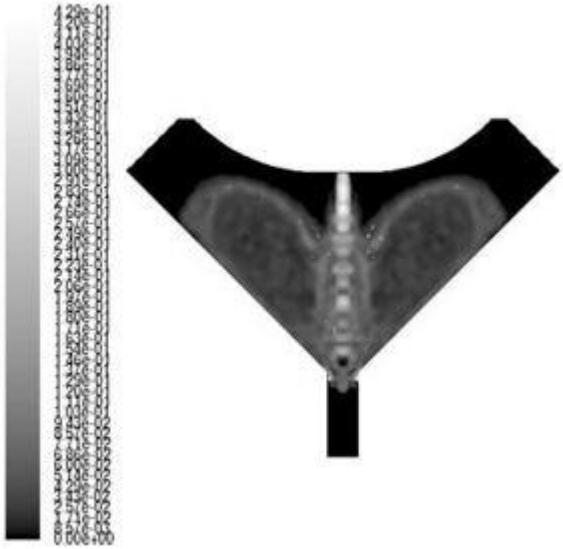

Figure 35. 2.0 seconds

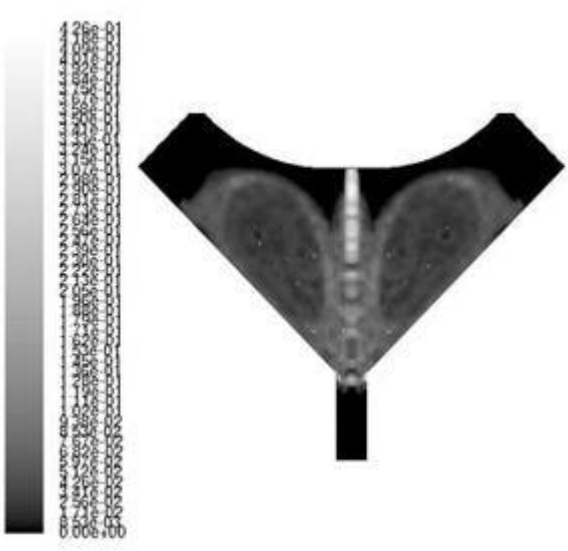

Figure 36. 2.3 seconds

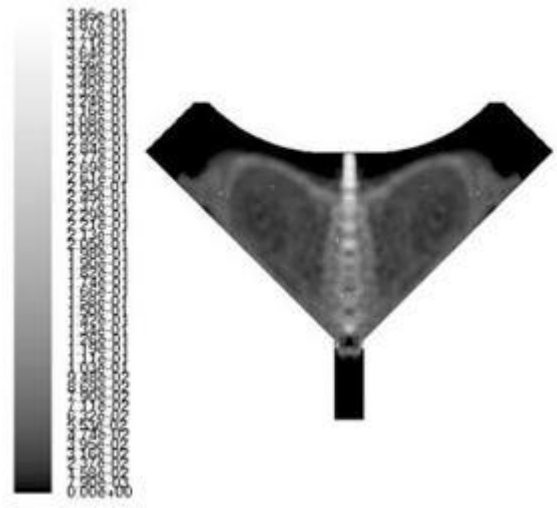

Figure 37. 2.6 seconds